Investigation of a deep ice core from the Elbrus Western Plateau, the Caucasus, Russia

V. Mikhalenko[1], S. Sokratov[2], S. Kutuzov[1], P. Ginot[3,7], M. Legrand[3], S. Preunkert[3], I. Lavrentiev[1], A.Kozachek[4], A.Ekaykin[4,6], X. Faïn[3], S. Lim[3,9], U. Schotterer[5,a],V. Lipenkov[4], and P. Toropov[1,8]

[1]Institute of Geography, Russian Academy of Sciences, Moscow, Russia
[2] Arctic Environment Laboratory, Faculty of Geography, Lomonosov Moscow State University, Moscow, Russia
[3]Univ. Grenoble Alpes, CNRS – UMR5183, Laboratoire de Glaciologie et Géophysique de l'Environnement (LGGE), Grenoble, France
[4]Arctic and Antarctic Research Institute, St. Petersburg, Russia
[5]Climate and Environmental Physics Group, University of Bern, Bern, Switzerland
[6] St. Petersburg State University, St. Petersburg, Russia
[7] Observatoire des Sciences de l'Univers de Grenoble, IRD UMS222, CNRS, Université Joseph Fourier Grenoble 1, Saint Martin d'Héres, France
[8] Department of Meteorology and Climatology, Faculty of Geography, Lomonosov Moscow State University, Moscow, Russia
[9] Department of Earth and Environmental Sciences, Korea University, Seoul, South Korea

[a] Retired

Correspondence to: V. Mikhalenko (mikhalenko@hotmail.com)

Abstract

A 182 meter ice core was recovered from a borehole drilled to bedrock on the Western Plateau of Mt. Elbrus (43°20′53.9″N, 42°25′36.0″E; 5115 m a.s.l.) in the Caucasus, Russia in 2009. This is the first ice core in the region that represents a paleoclimate record that is practically undisturbed by seasonal melting. Relatively high snow accumulation rates at the drilling site enabled analyzing the intra-seasonal variability in climate proxies. Borehole temperatures ranged from −17 °C at 10 m depth to −2.4 °C at 182 m. A detailed radio-echo sounding survey showed that the glacier thickness ranged from 45 meters near the marginal zone of the plateau up to 255 m at the glacier center. The ice core has been analyzed for stable isotopes ($\delta^{18}O$ and δD), major ions (K^+, Na^+, Ca^{2+}, Mg^{2+}, NH_4^+, SO_4^{2-}, NO_3^-, Cl^-, F^-), succinic acid ($HOOCCH_2COOH$), and tritium content. The mean annual net accumulation rate of 1455 mm w.e. for the last 140 years was estimated from distinct annual oscillations of $\delta^{18}O$, δD, succinic acid, and NH_4^+. Annual layer counting also helped date the ice core, agreeing with the absolute markers of the tritium 1963 bomb horizon located at the core depth of 50.7 m w.e. and the sulfate peak of the Katmai eruption (1912) at 87.7 m w.e. According to

mathematical modeling results, the bottom ice age at the maximum glacier depth is predicted to be ~660 years BP. The 2009 borehole is located downstream from this point, resulting in an estimated basal ice age of less than 350–400 years BP at the drilling site. The glaciological and initial chemical analyses from the Elbrus ice core help reconstruct the atmospheric history of the European region.

1 Introduction

Understanding climate change, regional environmental patterns, and predicting future impacts are currently some of the most important scientific challenges. The Earth's climate system has a profound influence on society and human prosperity. Discriminating human-induced and natural climate variability is an urgent task and cannot be solved by only using short instrumental meteorological observations or climate modeling experiments. Proxy records such as lake and marine sediments, ice cores, tree rings, corals can extend the instrumental climatic records. Some proxies have seasonal to annual resolution, and can be combine into large networks covering continental and even global scales. Individual proxies can be calibrated with instrumental data resulting in time series appropriate for statistical analyses and numerical modeling. Due to both the urgency of climate change, and our increased ability to synthesize paleoclimate data with future projections, it is essential to have reliable regional paleoclimate reconstructions for the last millennia (Vaughan et al., 2013). The study of chemical impurities in glacier snow and ice permit reconstructing our changing atmosphere from the pre-industrial era to present-day (see Legrand and Mayewski, 1997 for a review).

Ice cores from polar glaciers that result in multi-millennial records due to minimal disturbance by melt/refreeze processes are presently considered to be the best representation of past climate conditions at hemispheric scales. However, calculations based on observational data trends in the major climatic characteristics show highly pronounced regional variability. Such variability is reproduced by modern climate models and can be projected into the future (AMAP, 2011), but the reliability of the simulations depends on the amount and the quality of existent data and some of the results such as the precipitation rate are questionable (Anisimov and Zhil'tsova, 2012).

The need for regional paleoclimate records from non-polar areas has led to the development of numerous reconstructions of annual and seasonal resolution based on instrumental climate data and paleoclimate proxies. Ice cores from low and mid-latitude high mountain glaciers can reconstruct past atmospheric conditions in areas with long human histories. A number of studies examined climate and environmental changes in various non-

77 polar areas (Vimeux et al., 2009; Thompson, 2010) including the European Alps (Barbante et
78 al., 2004; Preunkert and Legrand, 2013; Schwikowski, 2004), the continental Siberian Altai
79 (Eichler et al., 2011), and Kamchatka (Kawamura et al., 2012; Sato et al., 2014).
80 Climate records located in the region of interest often best represent the climate
81 variability from the region itself. Despite their temporal length and their continuous records,
82 the Greenland and Antarctic ice core data are from sites that are very remote from most
83 inhabited areas. Therefore, the comparable paleoclimate records derived directly from glaciers
84 in Europe and Asia are highly valuable. However, seasonal melting and water infiltration
85 distort the climate proxies recorded in firn and ice even at high altitudes in the Andes (Ginot
86 et al., 2010), Himalaya (Hou et al., 2013) and the low latitudes of the Arctic islands
87 (Kotlyakov et al., 2004).
88 The documented conditions (Tushinskii, 1968; Mikhalenko, 2008) near the top of Mt.
89 Elbrus suggest the possibility of a reasonably long climatic record in an ice core not affected
90 by melt water infiltration. Relatively high accumulation on the Western Plateau (Mikhalenko
91 et al., 2005) assures high temporal resolution of the ice core data with the possibility of
92 seasonal variations in the analytical results (Werner et al., 2000). Due to this combination of
93 factors, we were motivated to recover ice cores from the Western Plateau of Mt. Elbrus to
94 obtain natural archives that preserve environmental data associated with atmospheric
95 chemistry, dust deposition, biomass burning, anthropogenic emission and climate change in
96 the Caucasus (Mikhalenko, 2010). The aim of the Elbrus drilling project is to reconstruct past
97 climate and environmental changes for the Caucasian region from the ice core. Here, we
98 provide an overview of the existing geographical, glaciological, meteorological, and
99 climatological knowledge from the region, and then focus on the glaciological and glacio-
100 chemical characterization of a new drilling site located on the Western Plateau of Mt. Elbrus.
101 We use stable isotopes, glacial-chemical records and simplified thermo-mechanical modeling
102 to create a chronology for the 182 m Elbrus ice core. Finally, we present the possibilities to
103 develop the high-resolution regional paleoclimate reconstruction from this ice core.
104
105 **2 Previous investigations of the Caucasus and Elbrus**
106
107 **2.1 Geographical and glaciological characteristics of the Caucasus region**
108
109 The Caucasus are situated between the Black and the Caspian Seas, and generally trend east-
110 southeast, with the Greater Caucasus range often considered as the divide between Europe

and Asia. The glaciers in the Caucasus cover an area of around 1121±30 km^2 (Kutuzov et al., 2015) (Fig. 1).

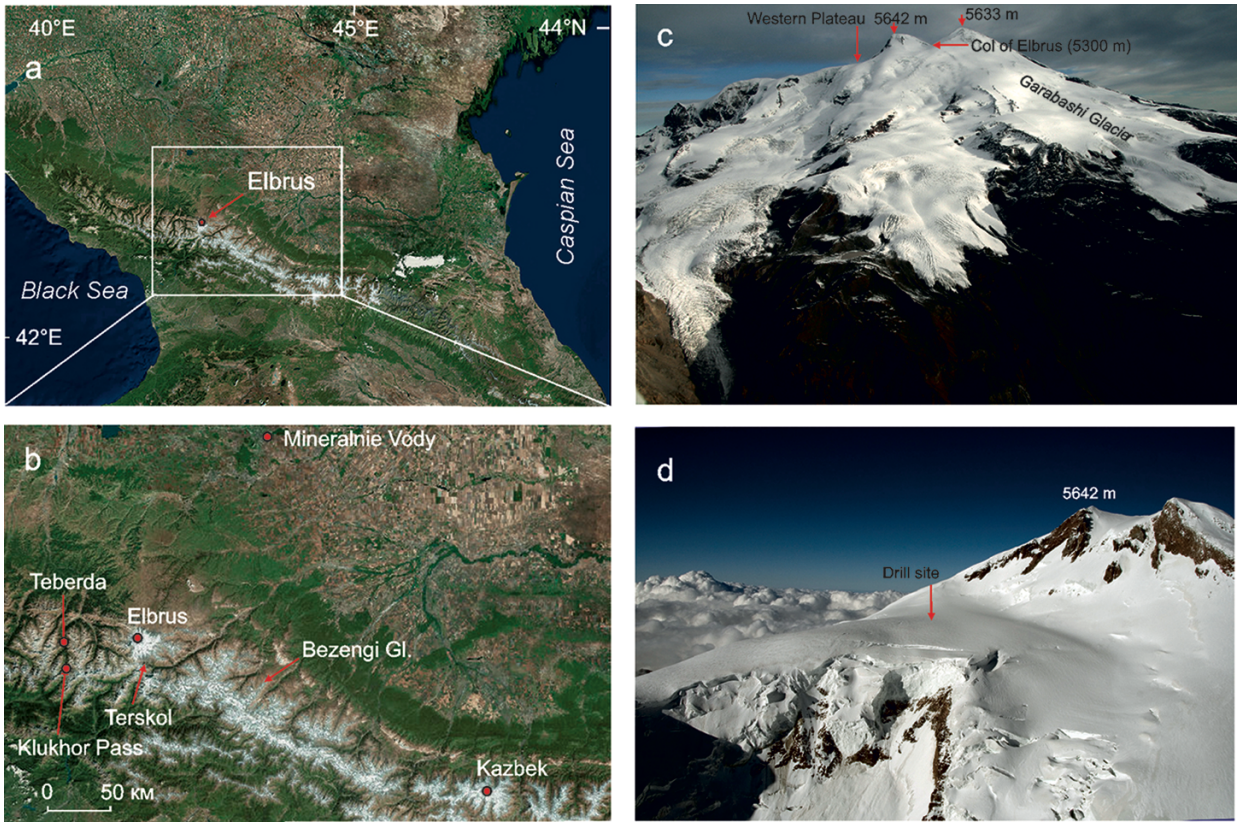

Figure 1. Location of study area: (a) Mt. Elbrus in the Caucasus;(b) glaciers and meteorological stations;(c) Mt. Elbrus from the south demonstrating the position of the Western Plateau;(d) Western Elbrus Plateau drill site (photos by I. Lavrentiev on September 2009). ArcGIS World Imagery basemap used as the background. Source: DigitalGlobe.

Glacier studies in the Caucasus began more than hundred years ago and mainly focused on glacier mapping (Pastukhov, 1893; Podozerskii, 1911) or reconstructing past glacier positions by geomorphological methods (Abich, 1875; Mushketov, 1882; Kovalev, 1961; Serebryannyi at el., 1984). Records of contemporary glaciological processes were obtained during the International Geophysical Year (IGY) in 1957–1959 (Tushinskii, 1968) when the climatic conditions of the glacial zone, accumulation and ablation of the glaciers, glacier runoff, glacier ice formation zones, and snow and firn stratigraphy were investigated. These studies were mainly conducted on the southern slope of Elbrus extending from the glacier tongue to the summit (Figure 1b) and determined that surface snow melting did not occur above 5000 m (Troshkina, 1968). Complex studies of mass, water, and the heat balance of glaciers in the Caucasus were started during the International Hydrological Decade (1964–1974) (Golubev et al., 1978; Dyurgerov and Popovnin, 1988; Krenke et al., 1988). A number

of studies examined fluctuations in glacier dimensions and volume (Stokes et al., 2006; Kutuzov et al., 2012, 2015; Nosenko et al., 2013, Shahgedanova et al., 2014), glacier mass balance (Rototaeva and Tarasova, 2000) and regional snow chemistry (Kerimov et al., 2011). Characteristics of the mineral dust and its source were investigated using shallow ice cores and snow pits records from Elbrus (Kutuzov et al., 2013; Shahgedanova et al., 2013).

In addition to the glaciological studies, multiple tree-ring based reconstructions represent mean summer air temperature, river run-off and glacier mass balance in the region (Dolgova et al., 2013; Solomina et al., 2012). The first regional lake sediment cores retrieved in 2010, 2012 and 2013 demonstrate an excellent potential for using lacustrine records to study long-term climate and glacier history variations (Solomina et al., 2013).

Despite the substantial glacier area in the Caucasus, few suitable sites for ice core research exist due to the relatively low elevation and considerable surface melting below 5000 m. Several shallow and intermediate depth ice cores have been recovered at the Caucasus glaciers (Golubev et al., 1988; Zagorodnov et al., 1992; Bazhev et al., 1998), but these previous studies were conducted at sites where considerable melt water percolation smoothed isotopic and geochemical profiles. However, the vast high-elevation plateaus on the glaciers of Elbrus (5642 m), Kazbek (5033 m), and Bezengi (~5000 m) (see Fig. 1b) present promising sites for obtaining ice-core records.

2.2 Geographical and glaciological characteristics of Elbrus

Elbrus, the highest summit of the Caucasus, contains two peaks at its highest elevations with both an eastern (5621 m a.s.l.) and western (5642 m a.s.l.) summit where the whole complex is covered by glaciers with a total area of 120 km^2 (Zolotarev and Khar'kovets, 2012) (Fig. 1). Elbrus is an active volcano but only minor fumarole activity is currently observed (Laverov et al., 2005).

Glaciers on Elbrus are situated in the altitudinal range from 2800 m to 5642 m. Stratigraphic records display several ice formation zones on Mt. Elbrus (Bazhev and Bazheva, 1964; Psareva, 1964; Troshkina, 1968). The coldest conditions occur above 5200 m a.s.l., where the mean summer air temperature does not exceed 0 °C while the Elbrus glaciers between 4700–4900 m a.s.l. have limited surface melting. Ice lenses up to 30 cm thick alternate with firn horizons in the uppermost snow and firn at 5050 m a.s.l. (Mikhalenko, 2008). Snow accumulation measurements from 1985 and 1988 demonstrate total snow accumulation of 400–600 mm w.e. a^{-1} with considerable wind-driven snow erosion at the col

of Elbrus (5300 m a.s.l.; Fig. 1c). The snow/firn temperature measured at a depth of 6 m was −14°C at the col, indicating absence of melt water runoff from this zone.

Long term (1983 to present) mass-balance records of the Garabashi glacier show negative values since 1994. Extremely high summer temperatures and glacier melting accompany this negative trend. The Garabashi glacier surface elevation has thinned by 3.2 m over the last decade near the equilibrium line (Nosenko et al., 2013).

A 76 m long ice core was recovered in the accumulation area of the Garabashi Glacier at 3950 m a.s.l.in 1988 (Zagorodnov et al., 1992). The firn in this ice cores completely transforms into ice as a result of melt water refreezing at 23–24 m depth. Thus, the geochemical profiles obtained from the ice core were smoothed by melt water percolation and could not be used for paleoclimate and environmental reconstruction.

The next ice core drilled in this region was recovered on the Western Plateau of Elbrus, at 5115 m a.s.l. (Fig. 1).The plateau area is ~0.5 km^2 and is bordered to the south and south-east by two lava ridges, and by a vertical wall of Mt. Elbrus to the east. The first ice core drilling campaign during July 4–6, 2004 resulted in a 21.4 m ice core with associated borehole temperatures and glacier thickness measurements (Mikhalenko et al., 2005). The 10-m depth temperature of −17°C indicated that any meltwater refreezes at only a few centimeters below the surface and thus isotopic and soluble ions profiles are preserved. Ice-core records of this first shallow ice core indicated good preserved seasonal stable isotopic ($\delta^{18}O$ and δD) oscillations and mean annual accumulation rates of approximately 1200 mm w.e.

2.3 Climatology of the Caucasus and Elbrus

The summer atmospheric circulation pattern in the Caucasus is dominated by the subtropical high pressure to the west and the Asian depression in the east. In the winter, circulation is affected by the western extension of the Siberian High (Volodicheva, 2002). The Caucasus are located in the southern section of the vast Russian Plain and are therefore buffeted by the unobstructed passage of cold air masses from the north. High elevation ridges in the southern Caucasus deflect air flowing from the west and south-west. The influence of the free atmosphere on the Elbrus glacier regime is significantly larger than local orographic effects as the glacier accumulation area lies above main ridges.

Most of the annual precipitation occurs in the western and southern sections of the Caucasus, reaching 3240 mm a^{-1} at Achishkho weather station (1880 m). Precipitation ranges between 2000 and 2500 mm a^{-1} at 2500 m a.s.l. in the west and declines to 800–1150 mm a^{-1} in the east on the northern slope of the Caucasus. Precipitation ranges from 3000–3200 mm

a^{-1} in the west to 1000 mm a^{-1}in the east for the southern macroslope. The proportion of winter precipitation (October–April) also declines eastward from more than 50 % to 35–40 % for the northern Greater Caucasus and from 60–70 % to 50–55 % for the southern slope (Rototaeva et al., 2006). The proportion of solid precipitation increases with altitude and reaches 100 % above 4000–4200 m. The altitude of the glacier equilibrium line (ELA), tends to increase from 2500–2700 m in the Belaya, Laba and Mzymta river basins in the west to 3700–3950 m in the Samur and Kusurchay basins in the eastern sector of the northern macroslope of the Caucasus.

Mean summer (May–September) air temperature at the ELA ranges from 6–7 °C in the west to 1–2 °C in the east. The ELA is much higher on the glaciers of the northern macroslope, especially in the central Caucuses, where the ELA on the northern slope of Elbrus is 1000 m higher than on Svanetia glaciers 80 km southward. The number of high-elevation meteorological stations is very limited in the Caucasus. Figure 2 shows the mean monthly air temperature and precipitation at the Klukhor Pass, Teberda and Terskol meteorological stations in the western and central Caucasus (Figure 1 and Table 1).

Table 1. Meteorological data used in this work (modified from Solomina et al., 2012)

Meteorological station	Geographical coordinates	Altitude, m	Beginning of observation
Klukhor Pass	N 43°15′; E 41°50′	2047	1956
Teberda	N 43°27′; E 41°44′	1313	1956
Terskol	N 43°15′; E 42°30′	2214	1951
Mineral'nye Vody	N 44°14′; E 43°04′	316	1955

Air temperatures at these stations are in good agreement and correlate well with lowland stations (r = 0.7–0.9, p<0.01), indicating the homogeneity of the temperature regime for the investigated area (Solomina et al., 2012). Variations in mean annual and monthly temperatures for the Klukhor Pass station for the period of observation (see Table 1) does not display a statistically significant trend. A positive trend for mean annual temperature (r=0.33, p<0.05) and a slight positive trend for summer temperature occurs at the Teberda station. Temperature records from the Terskol station located 7 km southward from the Elbrus glaciers show a negative mean annual temperature trend for the whole period of observation (r =−0.35, p<0.05) (Solomina et al., 2012) but mean summer (May–September) temperatures increased from 11.5 °C in 1987–2001 period to 12.0 °C over the last decade. Winter precipitation increased by 20% over the same period while summer precipitation did not show any change (Nosenko et al., 2013).

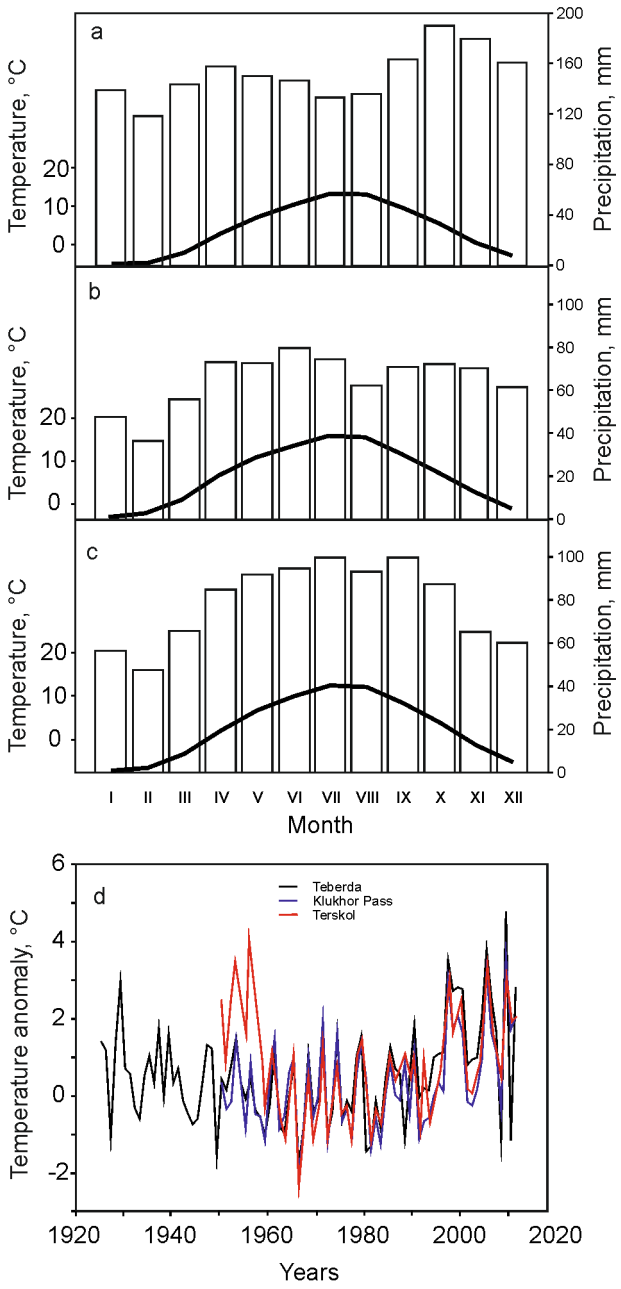

Figure 2. Mean monthly air temperature and precipitation at the Klukhor Pass (a), Teberda (b), and Terskol (c) meteorological stations and (d) anomalies of mean summer temperature with deviations from the mean 1961–1990 value.

The first meteorological measurements were taken on the Elbrus glaciers in 1934–1935 by an expedition of the USSR Academy of Sciences (Baranov and Pokrovskaya, 1936). Air temperatures, pressure, humidity, wind regime, and incoming solar radiation have been measured at four sites from Terskol at 2214 m a.s.l. to the col of Elbrus at 5300 m. A permanent meteorological station was established near Priyut–9 on the southern slope of the Garabashi Glacier at 4200 m a.s.l. in 1934. According to 1949–1952 data demonstrate a mean

annual air temperature of −9.2 °C. The temperature of the coldest month (January) was −17.1 °C while the July temperature was −0.5 °C. The minimum air temperature of −36.1 °C was measured on January 30, 1950, with a maximum of 10.7 °C on August 1, 1950. An annual precipitation rate of 1128 mm was observed for 1949–1952. The summer months (April–October) contribute 75% of the total precipitation, while the winter months (November–March) account for only 25% (Matyukhin, 1960). The maximum wind speed at Priyut–11 station of 56 m $s^{-1}$was measured in January 1952.

During the IGY (1957–1959) the permanent all-year meteorological station was established on the Glacier Base on the southern slope of the Elbrus at 3700 m a.s.l. Meteorological records from this site include diurnal air pressure and temperature, precipitation, humidity, cloudiness, wind regime and snow cover thickness (Tushinskii, 1968). Heat balance, air temperatures, wind speed were recorded during occasional observations in the col of Mt. Elbrus (5300 m). The first accumulation and ablation measurements on the southern slope of Mt. Elbrus were done during the IGY and in 1961–1962 (Bazhev and Bazheva, 1964).

3 The Western Elbrus Plateau glacier archive

In the following section we will present recent meteorological, glaciological and glacio-chemical investigations conducted on the Western Elbrus glacier plateau with the aim of obtaining knowledge about the suitability of this site to obtain atmospheric relevant ice core records.

3.1 On site meteorological measurements

An automatic weather station (AWS) from AANDERAA Data Instruments was installed on the Western Elbrus Plateau at 5115 m a.s.l. at the drill site in 2007. The AWS was working between July 30, 2007, and January 11, 2008, but disappeared afterwards under unascertained circumstances. Here we discuss records until October 12, 2007, comprising the period with uninterrupted, consistent data. Air temperature, wind speed and direction, humidity, air pressure, radiation balance, and snow cover thickness have been measured with the time resolution of 1 hour. According to AWS records, mean daily air temperatures were negative during the period of observations. Hourly-averaged temperatures were also negative while the maximum un-averaged air temperatures were recorded on eight occasions and ranged from 0.1 °C to 3.1 °C. Mean hourly-averaged wind speed on the drilling site was 2.9 m

279 sec^{-1}throughout the entire period of observation. Wind gusts up to 21.4 m sec^{-1} were observed
280 when fonts passed the station while the mean daily maximum wind speed was 6.7 m sec^{-1} in
281 August–September 2007. Our data did not cover the whole year but according to
282 measurements from 1961–1962 the average wind speed was approximately 30% higher in the
283 winter on the southern slope of Elbrus (Tushinskii, 1968). A combination of high snow
284 accumulation and the relatively low average wind speed from the prevailing westerlies allows
285 us to assume that most of the precipitation did not move far from its depositional site and was
286 not scoured by wind.
287 AWS records were compared with measurements from the mountain meteorological
288 station Klukhor Pass (2037 m a.s.l.; 50 km westward) and the lowland Mineral'nye Vody
289 station (316 m a.s.l.; 120 km north–eastward) (Table 1) as well as with the 20th century
290 Reanalysis V2 data provided by the NOAA/OAR/ESRL PSD, Boulder, Colorado, USA,
291 (http://www.esrl.noaa.gov/psd/) (Fig. 3 a, b). A temperature lapse rate of 0.6° per hundred m
292 elevation was observed during the summer months. In winter, however, the lapse rate
293 decreases due to temperature inversions at the Mineral'nye Vody station. There is a good
294 agreement between the temporal variations of mean daily air temperature measured by the
295 AWS at the drill site, 20th Century Reanalysis and other meteorological stations data
296 (r>0.85). Therefore the temperature variations at the West Elbrus plateau are consistent with
297 the regional temperature regime.
298

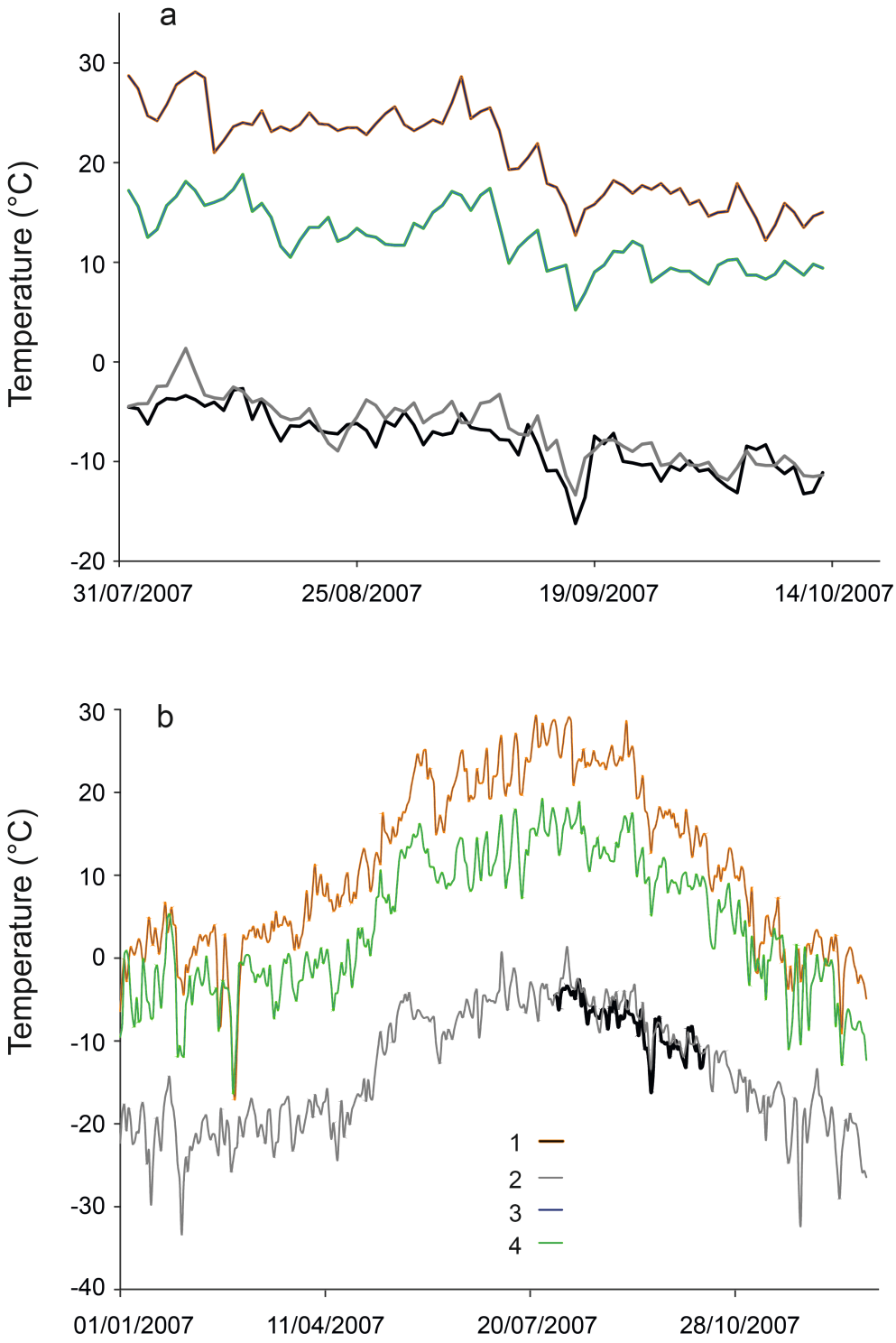

Figure 3. Daily temperature means (T, °C) for the periods of 1 August−12 October 2007 (a) and 1 January–31 December 2007 (b): 1 – AWS at the Western Elbrus Plateau; 2 – 20th Century Reanalysis V2; 3 – Mineral'nye Vody meteorological station; 4 – Klukhor Pass station.

In June 2013 we conducted meteorological observations on the Western Elbrus Plateau near the 2009 drilling site with an AWS DAVIS Vantage Pro 2 including air temperature, humidity and wind speed at 0.5 and 2.0 m with 15 min resolution (Figure 1 and 4). Along

with the estimation of eddy flux of heat and moisture, we measured the fluxes of total, scattered and reflected radiation. Meteorological conditions during the observation period encompassing the maximum insolation at the summer solstice were close to mean annual parameters. Downward shortwave radiation varied between 1 to 1.2 kW m^{-2} which is 73–88 % of the solar constant at the outer boundary of the atmosphere and 78–93 % of total insolation at 43°N latitude during that time of year. Albedo has a dominant role in the shortwave radiation balance. Mean albedo values of 0.66 were measured at the plateau in June 2013.

Initial measurements of radiation balance were conducted in Elbrus in 1968–1960 and showed that downward short wave radiation ranged from 1.1 kW m^{-2} at an elevation of 3750 m a.s.l. up to 1.2 kW m^{-2} at 5300 m a.s.l. (Tushinskii, 1968). Despite the negative air temperatures, the radiation balance was positive except for during the night. The mean value of the radiation balance encompassing both short-wave and long-wave radiation was 150 W m^{-2}, affecting surface melting and snow recrystallization.

3.2 Ground base survey: surface topography and radar sounding

Detailed measurements of ice thickness were carried out in 2005 and 2007 using the monopulse ice-penetrating radar VIRL with a central frequency of 20 MHz (Vasilenko et al., 2002, 2003). VIRL ice penetrating radar consists of a transmitter, receiver and digital recording system with GPS. In order to synchronize the transmitter and receiver we used a special radio channel with a repetition rate of 20 MHz. We modified the advanced VIRL–6 radar with an optical channel in 2007 (Berikashvili et al., 2006) allowing simultaneous recording and controlling. The time interval ranged between 1 to 99 sec for obtaining both radar and navigation data as well as for performing the hardware and program stacking (from 1 to 6192 times) of wave traces.

The average radio wave velocity (RWV) in firn and ice can calculate ice thickness from measured time delays of radar signals reflected from the bedrock. RWV depends on firn/ice density and temperature. We did not measure RWV (V) at the Western Elbrus Plateau, but calculated the result as a function of glacier depth (z) through measured ice core density $\rho_d(z)$ and borehole temperature T (z) profiles:

$$V(z) = c/[\varepsilon'(\rho_d, T)]^{1/2}, \quad (1)$$

where $c = 300$ m μs^{-1} – radio wave velocity in air; $\varepsilon'(\rho_d, T)$ – dielectric permeability of snow, firn and ice as a function of density $\rho_d(z)$ and temperature $T(z)$ (Macheret, 2006). $\varepsilon'(\rho_d)$ was calculated for two component dielectric mixture of ice and air (Looyenga, 1965):

$$\varepsilon'(\rho_d, T) = \{(\rho_d/\rho_i)[\varepsilon'_i(T)^{1/3} - 1] + 1\}^{1/3}, \quad (2)$$

where $\rho_i = 917$ kg m^{-3} – density of glacier ice. $\varepsilon'_i(T)$ was calculated from (Mätzler and Wegmüller, 1987):

$$\varepsilon'_i(T) = 3.1884 + 0.0091\ T. \quad (3)$$

The average RWV of 180 m μs^{-1} was calculated for the 181.8 m ice thickness at the drilling site taking into account the depth variations from ρ_d and T and the measured time delay of radio signal to ice thickness at each point.

We combined two data sets, from 2005 and 2007 to construct an ice thickness map. In total, we measured the glacier depth at more than 10,000 sounding points along 6.5 km profiles with an estimated accuracy of ice thickness measurements of 3% (Lavrentiev et al., 2010). The maximum depth was 255±8 m at the central part of the plateau, with minimum values of about 60 m near the edge. Radar records and digital elevation model ASTER GDEM averaged for 2000–2009 map the bedrock topography (Fig. 4). ASTER GDEM with an error of ±20 m (ASTER…, 2009) is in a good agreement with the 1959 Northern Caucasus topographic map and the 1997 digital orthophotomap of Elbrus (Zolotarev and Khar'kovets, 2000).

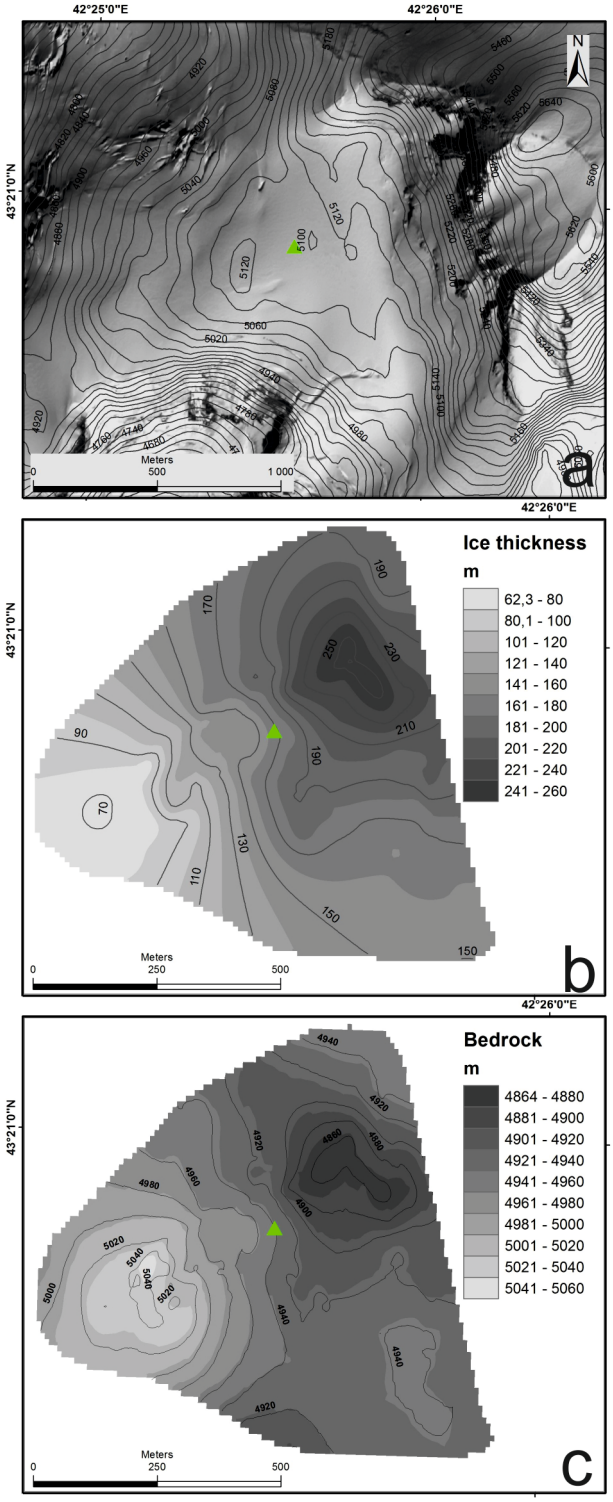

Figure 4. Glacier surface (a), ice thickness (b), and bedrock relief (c) on the Western Elbrus Plateau. The green triangle marks the position of the drilling site.

3.3 Ice core drilling and analysis

3.3.1 Methods

Due to the promising glacier archive conditions obtained from the shallow ice coring in 2004 (see section 2.2), a full-depth ice core drilling was completed on the Western Plateau from

August 27 to September 6, 2009 (Mikhalenko, 2010). Bedrock was reached at the depth of 181.80 m. Drilling was done in a dry borehole using the lightweight electromechanical drilling system developed by Geotech Co. Ltd., Nagoya, Japan. Technical details of the drill are described in (Takeuchi et al., 2004). The recovered ice cores were subjected to stratigraphic observations, packed into plastic sleeves and stored in a snow pit with temperatures of −10 °C. Ice core drilling was accompanied by borehole temperature measurements (using thermistor chains which were left for three days in the borehole and calibrated before and after the study with an error of ±0.1°C), and snow pit sampling conducted 30 m to the south of the drilling site. The ice core was shipped in frozen condition to the cold laboratory of the Lomonosov Moscow State University where detailed stratigraphic descriptions including photographing of each piece of the core and bulk density measurements were conducted.

In addition to the 2009 deep ice core a subsequent 12-meter ice core was extracted in June 2012 at the same site to expand the existing ice core sample set from 2009 to 2012. The 2012 ice core was also used for the dust study of Kutuzov et al. (2013). Finally, in June 27 to 30, 2013, a 20.36 m ice core was recovered at the same location.

Stratigraphic descriptions of the ice core were carried out using transmitted-light illumination resulting in 1 mm resolution details of the depths and thickness of individual horizons. The density of firn and ice were measured on 457 individual samples. Figure 5 shows the bulk density distribution with depth. The sharp random outliers from the general profile, especially with the lower values, could result from uncertainties in estimations of samples lengths. The uncertainty increases for the denser and smaller samples.

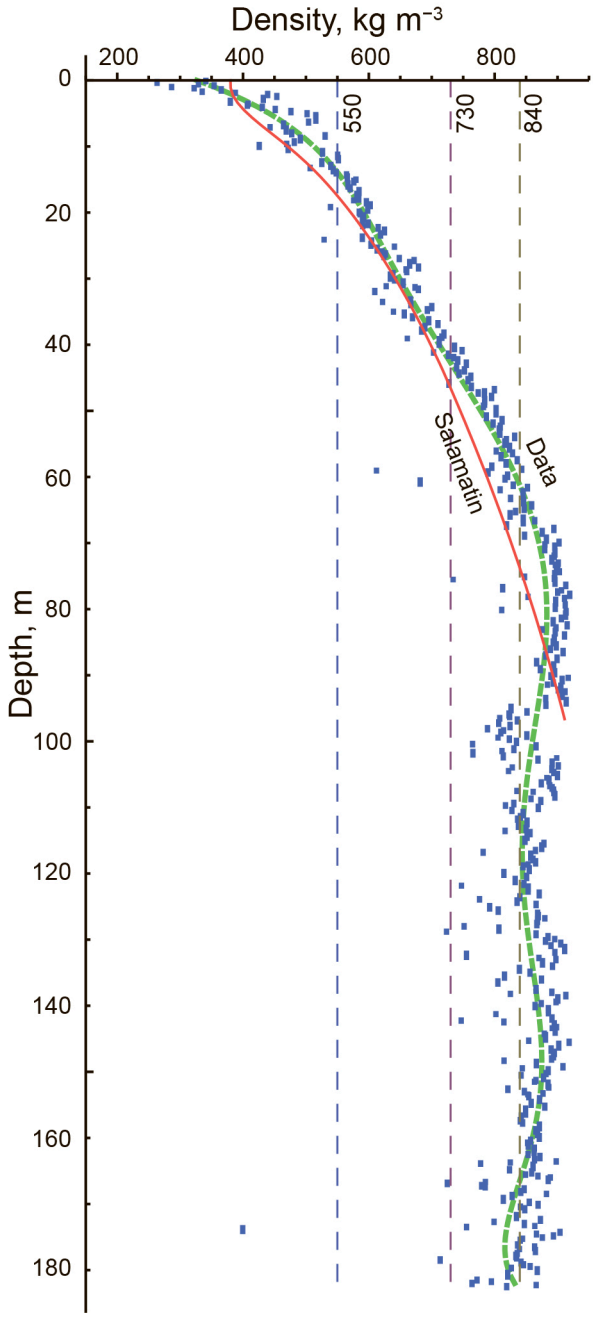

Figure 5. Measured (blue dots) and simulated (red line) ice core density profile with critical densities shown as dashed lines (see 3.3.2.). The green dashed line is a running mean for the measured density values.

Ionic species such as ammonium (NH_4^+) succinate ($HOOCCH_2COO^-$, also denoted succinic acid) were investigated along the uppermost 157 m of the Elbrus core (122 m w.e.) with the aim of aiding in ice core for alpine firn and ice samples (Legrand et al., 2007a). Pieces of firn and ice were decontaminated in a clean air bench located in a cold room using a pre-cleaned electric plane tool. A total of 3350 subsamples were obtained along the 157 m with a sample resolution decreasing from 10 cm at the top to 2 cm at 157 m depth.

For cations (Na^+, K^+, Mg^{2+}, Ca^{2+}, and NH_4^+), a Dionex ICS 1000 chromatograph

equipped with a CS12 separator column was employed. For anions, a Dionex 600 equipped with an AS11 separator column was used with an eluent mixture of H_2O, NaOH at 2.5 and 100 mM and CH_3OH. A gradient pump system allows determining inorganic species (F^-, Cl^-, NO_3^-, and SO_4^{2-}) as well as short-chain monocarboxylates (denoted $MonoAc^-$) and dicarboxylates (denoted $DiAc^{2-}$). For all investigated species, ion chromatography and ice core decontamination blanks were found to be insignificant with respect to respective levels found in the ice core samples.

As will be discussed in greater detail in section 3.3.5, the search for volcanic horizons in the Elbrus ice cores requires examining the acidity (or alkalinity) of samples by evaluating the ionic balance between anions and cations where concentrations are expressed in micro-equivalents per liter, $\mu Eq\ L^{-1}$):

$$[H^+] = ([F^-] + [Cl^-] + [NO_3^-] + [SO_4^{2-}] + [MonoAc^-] + [DiAc^{2-}]) - ([Na^+] + [K^+] + [Mg^{2+}] + [Ca^{2+}] + [NH_4^+]) \quad (4)$$

Within the present study, we focus (section 3.3.4) on the NH_4^+ and succinic acid profiles, in order to (1) define a criterion which allows separating winter and summer snow deposition and (2) to apply this criterion to the first 157 m of the Elbrus ice core in order to establish a depth-age relationship based on both annual layer counting and the NH_4^+ and succinic acid depth profiles.

The shallow 2012 and 2013 ice cores and the deep (down to 106.7 m) 2009 ice core were analyzed for deuterium-hydrogen (D/H) and oxygen ($^{18}O/^{16}O$) isotope ratios using a Picarro L1102-*i* instrument in the Climate and Environmental Research Laboratory (CERL), Arctic and Antarctic Research Institute, St. Petersburg, Russia. The instrument was calibrated on a regular basis with the isotopic standards V-SMOW, GISP and SLAP provided by the International Atomic Energy Agency (IAEA) to estimate the precision of the measurements and to minimize the memory effect associated with continuous measurements. The reproducibility of the measurements was ±0.07 ‰ for oxygen isotopes ($\delta^{18}O$) and ±0.3 ‰ for deuterium (δD). The CERL laboratory work standard SPB was measured after every 5 samples. The $\delta^{18}O$ and δD values are expressed in ‰ units relative to the V-SMOW value.

3.3.2 Borehole temperatures

Figure 6 shows the vertical temperature profile measured along the 181 m long borehole drilled in 2009. Temperatures ranged from −17 °C at 10 m depth to −2.4 °C at 181.8 m. The

temperature profile can be divided into three parts based on different temperature gradients: from the surface down to 10 m, from 10 m to 100 m, and from 100 m to the glacier bottom. The upper section of the temperature profile reflects seasonal changes at the surface. The borehole temperature ranges from −17 °C to −12 °C between 10–100 m, and most accurately reflects past temperature fluctuations. Temperature changes are almost rectilinear from 100 m depth to the glacier bottom and provide evidence of a steady heat transfer regime. The heat flux of 0.34 W m^{-2} at the glacier bottom was calculated from measured temperature gradient and the coefficient of heat conductivity of ice (2.25 W m^{-2}). This value is 4–5 times higher than the average heat flux density for the Earth's surface and higher than the mean value for Central Caucasus, and may be associated with heat magma chamber of the Elbrus volcano. Fig. 6 also shows the temperature profile measured in the 19 m borehole in 2013 and temperature records obtained in 2004 after the 22-m depth shallow ice core drilling on the Western Plateau (Mikhalenko et al., 2005). The good match between records is indicative of the stable temperature regime on the Western Elbrus Plateau for the last decade.

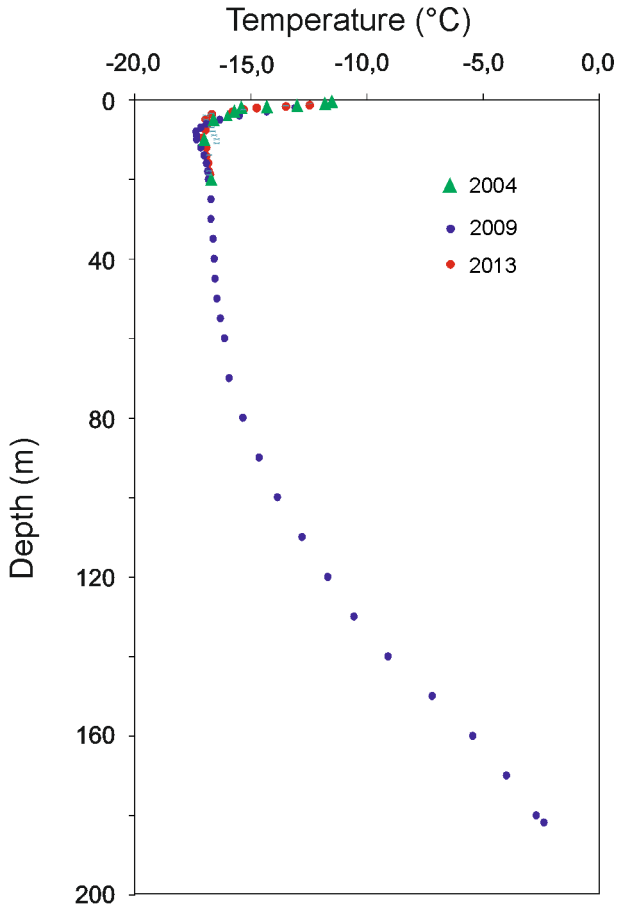

Figure 6. Measured temperature profiles at the Western Elbrus Plateau drill site for different dates: green triangles = 22 m depth borehole drilled in 2004, blue dots = main 2009 borehole, and red dots = 20 m depth borehole drilled in 2013.

Using the altitudinal temperature gradient estimated in section 3.1 based on Western Plateau AWS temperature data close to the 2009 drill site and the low elevation station Mineral'nye Vody, we estimate the annual mean air temperature at the drill site is approximately −19°C. This value is close to the mean annual air temperature of −19.4 °C calculated using the general relationship with the ice temperature at the bottom of the active layer (Zagorodnov et al., 2006) and only slightly enhanced compared to the 10 m firn temperatures.

The measured temperature profile shows that basal melting can occur due to ice pressure at the deepest part of the glacier. Potential bottom melting has been estimated using a mathematical model of temperature regimes (Salamatin et al., 2001). Our modeling results demonstrate that basal melting occurs under ice thickness more than 220 m and but that its value does not exceed 10 mm w.e. y^{-1}.

3.3.3 Bulk density and ice core stratigraphy

The bulk density profile suggests a change in densification around the critical densities (Maeno and Ebinuma, 1983) of 550 and 840 kg m^{-3}, and no visible change at 730 kg m^{-3}, which is consistent with other analyses of density profiles (Hörhold et al., 2011; Ligtenberg et al., 2011). However, the slight decreasing trend in density at depths below the maximum values at ~80 m (Fig. 5), close to the critical density across the whole depth interval, is unlikely to be a systematic error in measurements and needs further investigation. Future research should account for the ice flow characterization and the possible effects related to the "intervening depth interval" (the alternation of layers which have already reached the close-off density, with layers that are still permeable) due to seasonal (Bender et al., 1997) or wind induced (due to seasonal differences in wind speeds) snow density variability at high accumulation sites. Unlike polar ice cores where the "intervening depth interval" is just a fraction of the whole length of the ice core (Bender et al., 1997), the measured bulk density in the Elbrus ice core spans a wide interval between 800 kg m^{-3} and 915 kg m^{-3} towards the bottom of the glacier (Figure 5). Comparing Elbrus's density profile with the results from the Salamatin et al. (2009) densification model demonstrates that there is an increase in the accumulation rate over the past several years. The minimum deviation between simulated and measured ice-core density profiles occurred when the assuming that the accumulation history was similar to the long-term precipitation changes observed at meteorological stations (Nosenko et al., 2013).

According to the morphogenetic classification of stratigraphic features (Arkhipov et al., 2001) two distinct types of layering were observed in the core: firn layers which have not been affected by melting, and ice layers formed by the refreezing of melt water in the surface snow. The thickness of the infiltration ice layers, which do not form every year, does not exceed 10 mm. Ice formation occurs in cold, dry conditions, as already concluded on the basis of borehole and air temperatures at the drill site (see sections 3.1 and 3.3.2). The pore close-off depth occurs at around 55 m, where the air bubbles separate from the surrounding ice matrix became separated. This depth coincides with a measured bulk density of around 840 kg m^{-3}. This density is consistent with the presence of ice layers as these layers increase the close-off density value above what is expected in ice in which no melting occurs (i.e. 830 kg m^{-3}).

3.3.4 Seasonal ice core stratigraphy of stable water isotopes

The seasonal cycle of the isotopic composition is detectable over the entire measured part of the core (Fig. 7). Mean seasonal values of δD are −200‰ for the winter and −25 ‰ for the summer. Values of $\delta^{18}O$ are about −5 to −10 ‰ in summer and −30 ‰ in winter. Using isotope values to determine annual cycles over 106.7 m of the ice core suggests that these 106.7 m covers 86 years (1924–2009 AD). The mean accumulation rate for this period based on this dating and taking into account the firn density and layer thinning was 1455 mm w.e. Figure 7 shows results of isotopic measurements of four different ice cores obtained from the Western Elbrus Plateau. While 2009, 2012 and 2013 cores were obtained from almost the same location; the 2004 core was drilled 120 m to the south-west. Good agreement in isotopic variations of all cores suggests a relatively homogeneous snow deposition on the plateau.

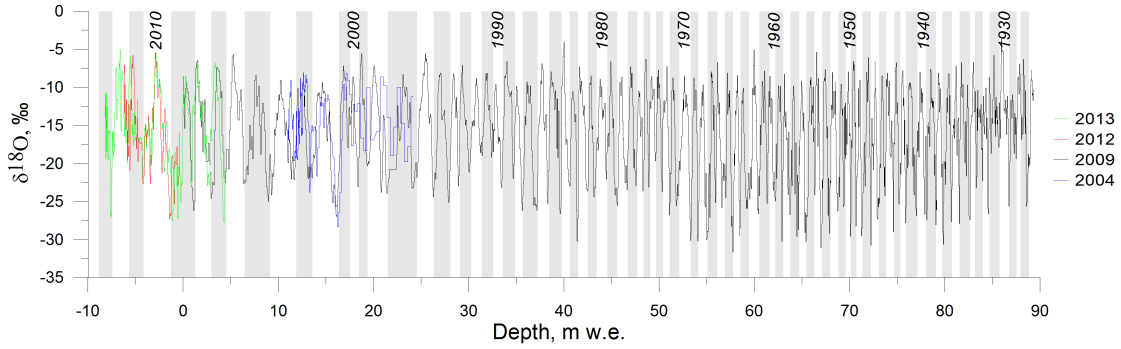

Figure 7. $\delta^{18}O$ profiles of the cores obtained in 2004, 2009, 2012, 2013. 0 m depth corresponds to the 2009 surface. Grey and white boxes depict annual layers.

We used the isotope diffusion model of Johnsen et al., 2000 to estimate the preservation of the isotopic signal with diffusive smoothing. Although the drilling site is located in a relatively warm place (−17 °C), the high snow accumulation rate does not favor strong diffusion, since any firn layer rapidly reaches the pore close-off depth. The maximum "diffusion length" at the pore close-off depth is estimated as 5 cm in ice equivalent (i.e.). The effective diffusion length may be even smaller if we take into account the ice lenses in the firn that prevent the vertical exchange of the water molecules.

Such a diffusion length means that all oscillations shorter than 13 cm i.e. will be completely erased due to the diffusion, while oscillations between 13 and 70 cm i.e. will survive but will be damped to some extent, and the cycles longer than 70 cm (e.g., the annual cycle) i.e. will not be affected by the diffusion. Thus, if during a single snowfall results in a 35-cm snow layer (that corresponds to 13 cm in i.e.), the isotopic signal of this layer will survive during the diffusion processes and will be seen in the ice core.

Diffusion occurs below the pore close-off depth, but the in ice is much slower than in firn. The final diffusion length solely depends on the time and temperature of the firn-ice thickness. Even if we take a maximum possible temperature (−2.4 °C) and an age estimate of a few hundred years, the additional diffusion in ice will still be very small. This combination leads us to an important conclusion; we may expect to obtain seasonal cycles in the isotope profile down to the very bottom of the core, and our ability to detect the annual cycle in the core depend on the sampling resolution, as well as on such basal processes such as layer folding and mixing.

3.3.5 Seasonal ice core stratigraphy of chemical parameters and ice core dating based on annual layer counting

We attempted to date the core by counting annual layers based on chemical ice core stratigraphical records, as we previously successfully applied such layer counting to mid-latitude Alpine ice cores using the NH_4^+ signal (Preunkert et al., 2000). Since NH_4^+ experiences strong maximum emissions in phase with strengthened summer upward transport of air masses, a particularly well-pronounced seasonal cycle is expected, such as observed at the Col du Dôme Alpine site (Preunkert et al., 2000; Fagerli et al., 2007). However, it appears that the NH_4^+ seasonal cycle at Elbrus is less pronounced than in the Alps. Whereas recent summer NH_4^+ levels are comparable at both sites, recent winter concentrations at Elbrus are significantly higher than at Col du Dôme.

The first study regarding the seasonality of Elbrus snow accumulation was conducted by Kutuzov et al. (2013) along a short firn core spanning the years 2012–2009. Based on the dust

562 layer stratigraphy of absolute-dated dust events and the stable isotope record the authors
563 showed that the annual deposition at Elbrus has a mean $\delta^{18}O$ signature of −15 ‰. The isotopic
564 signature consists of nearly equal deposition amounts from the warm season (45 % of total
565 accumulation), where $\delta^{18}O$ values vary between −5.5 ‰ and −10 ‰, and from the cold season
566 (55 % of total accumulation), for which values vary between −17 ‰ and −27 ‰.
567 The concentration distribution of NH_4^+ values was inspected in recent firn layers (0–12
568 mw.e.), and the 50 % concentration limit of 100 ppb was a first approach to separate snow
569 deposition arriving from summer and winter precipitation at Elbrus. However this criterion is
570 not conserved in time as the NH_4^+ sources are mainly anthropogenic in origin, with an
571 expected NH_4^+ trend in summer as well as in winter over the last 100 years. Therefore, a
572 second criterion was used to confirm our winter snow selection. This criterion used succinic
573 acid, a light dicarboxylic acid with an observed strong summer maximum and an almost non-
574 existent winter level exists in the current atmosphere in Europe (Legrand et al., 2007b). The
575 very low winter levels are related to the absence of source as this species is mainly
576 photochemically produced from biogenic precursors. The concentration distribution of
577 succinate values was inspected in recent firn layers (0–12 mw.e.), and the 50 % concentration
578 limit of 5 ppb separates snow deposition arriving from summer and winter precipitation at
579 Elbrus. Winter snow and ice layers were identified when both ammonium and succinate
580 criteria were fulfilled for more than 2 successive samples.
581 Figure 8 a, shows the result of this data dissectionover the uppermost 12 m w.e. along
582 with the $\delta^{18}O$ record (Fig. 8 e). The mean $\delta^{18}O$ level of selected winter data is −19.6 ‰, and
583 as demonstrated in Fig. 8 a, c the winter season selected from ammonium and succinate
584 concentrations matches quite well with winter sections deduced from the $\delta^{18}O$ profile.
585 However, when examining the $\delta^{18}O$ variability compared to the major ions it appears that
586 sometimes the spring season or even the beginning of the summer season may be included.
587 For dating by annual layer counting this shortcoming is not critical, however if the dataset is
588 inspected at seasonal resolution this definition of the spring season might be a handicap. In
589 this case a stronger criteria (NH_4^+<50 ppb and succinate < 3 ppb) may be applied in addition
590 to assure that only deposition corresponding to winter precipitation and associated
591 atmospheric background conditions are selected within the winter period. The mean $\delta^{18}O$
592 level of winter data selected using this criteria is –21.1 ‰, whereas seen in Figure 8a, c, and e
593 this selection may omit some winter seasons.
594

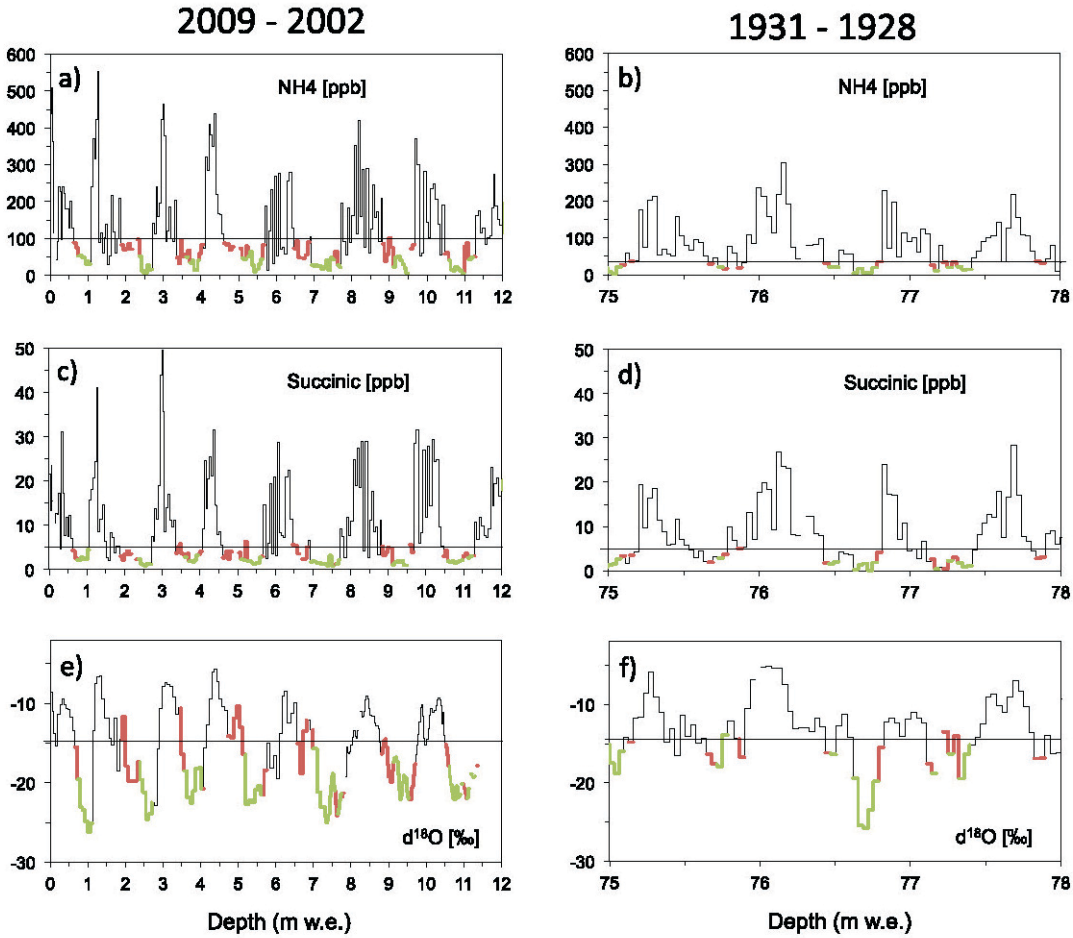

595

596 Figure 8. Seasonal variations in $NH4^+$ (a, b), succinic acid (c, d), and $\delta^{18}O$ (e, f) for different
597 sections of the Elbrus ice core. Red sections demonstrate winter samples based on the
598 following criteria: Succinic acid less than 5 ppb, NH_4^+less than 100 ppb for recent years and
599 less than 50 ppb prior to 1950.Green sections meet the following winter-background criterion:
600 Succinic acid less than 3 ppb, NH_4^+less than 50 ppb for recent years and less than 20 ppb prior
601 to 1950. Black bars in ionic plots refer to the winter criteria. The black bars in the $\delta^{18}O$ plots
602 refer to the respective mean value.

603

604 Examination of NH_4^+ and succinate minima below a depth of 12 m contrasts with
605 results from the European Alps, where in Elbrus the NH_4^+ winter level decreases significantly
606 from near the surface to around 70 m w.e. depth (see Fig. 8). Therefore, the NH_4^+ winter and
607 background criteria had been adjusted, using a winter (background) threshold of 50 ppb (30
608 ppb) from 52 – 62 m w.e. of the core and 30 ppb (20 ppb) from below a core depth of 62 m
609 w.e. In contrast, the succinate winter levels did not change and the 5 ppb criterion applied in
610 recent times was also applied in deeper layers. Fig. 8b, d, and f showed a comparison of
611 NH_4^+, succinate with the $\delta^{18}O$ record between 75 and 78 m w.e. (i.e. from 1931–1928 AD).
612 The winter criteria matches well with recent winter deposition as deduced from the stable

613 isotope content, although the stable isotope record tends to already be a bit smoothed
614 compared to the uppermost firn layers. As observed for the uppermost core section, we cannot
615 exclude that the winter criteria includes parts of an intermediate season, whereas the
616 background criteria selects only deposition arriving from the coldest precipitation.
617 Figure 9 shows the result of the dating of the Elbrus ice core. In addition to model
618 calculations detailed in section 3.4, the depth-age scale obtained by annual layer counting
619 using the $NH_4^+$and succinate criteria is reported down to 122 m w.e. Annual layer counting
620 was achieved as described above down to 85 m w.e. Below 85 m w.e., winter levels became
621 rather thin due to annual layer thinning but also likely due to upstream effects as commonly
622 encountered on such small-scale glaciers (Preunkert et al., 2000). Therefore, below 85 m w.e.
623 ice core layers in which less than 3 samples have reached the winter criteria were considered
624 as winter seasons, and from 113 to 122 m w.e. winter layers were also assigned when only
625 one of the two criteria was fulfilled for at least one sample while the other sample showed
626 only a relative minima that sometimes exceeded the fixed threshold. This lack of sharp
627 minima could be either due to the fact that winter sections become smaller than our sampling
628 resolution of 2–3 cm applied to core depths below 90 m w.e., and/or could be the result of an
629 incomplete precipitation preservation due to wind erosion upstream of the borehole as
630 observed on other small-scale Alpine glacier sites (e.g. Preunkert et al., 2000). In this latter
631 case a systematic lack of winter snow accumulation would occur in the deeper ice core layers.
632

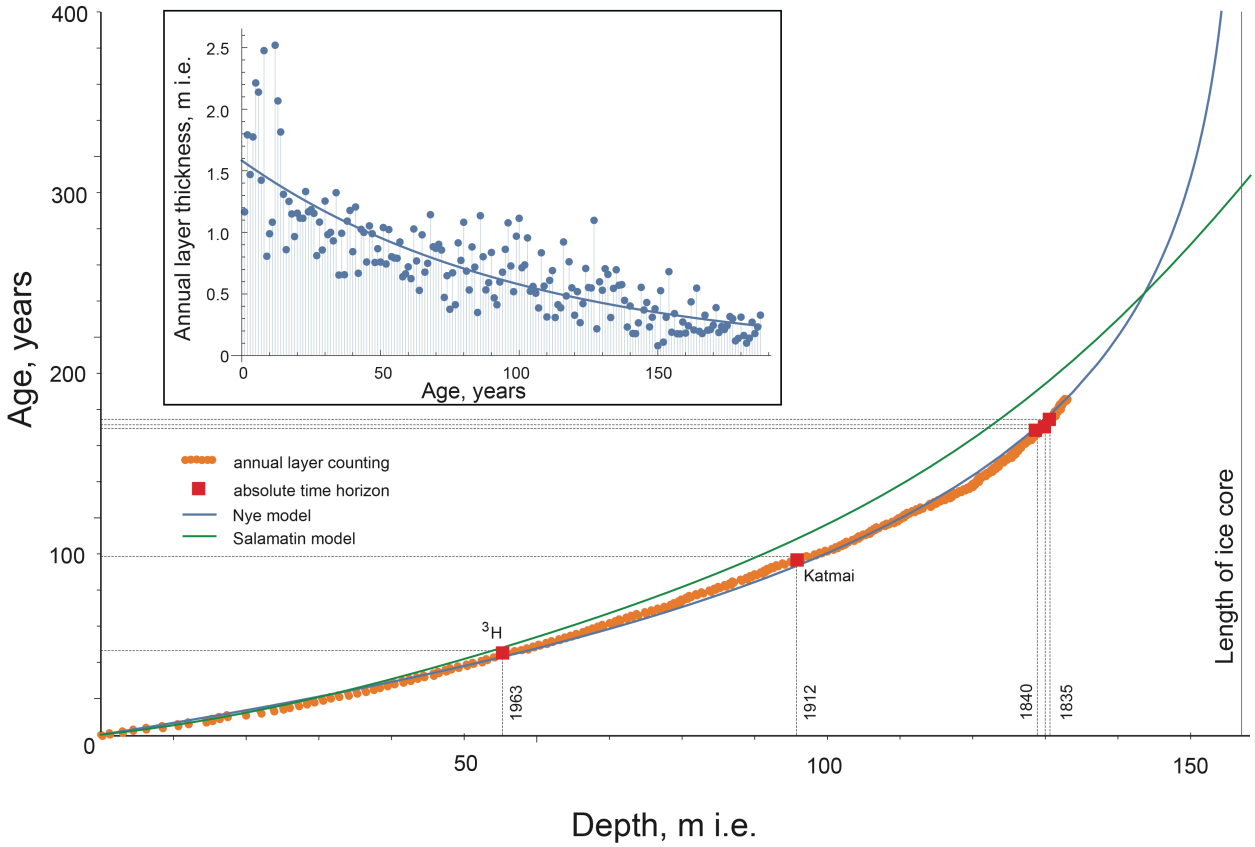

Figure 9. Depth (in m of ice equivalent)/age relation established for the Elbrus ice core by annual layer counting along the depth profile using ionic species (orange dots), and applying the ice flow models: Nye (blue line), Salamatin (green line). The insert represents the annual layer thickness (in m of ice equivalent) and the "Nye" least square fit (see text).

Dating based on annual layer counting of the chemical stratigraphy agrees fairly well with the 1963 AD tritium time horizon located at the core depth of 50.7 m w.e. and which is dated at 1965 AD using the ammonium stratigraphy, Fig. 10a. The layer counting results fits well with the dating achieved to 106.7 m based on the seasonal stratigraphy of the stable isotope profile. Whereas stable isotopes predict the year 1924 AD at a core depth of 106.7 m, the chemical stratigraphy leads to an estimate of the year 1926 AD at this depth.

To anchor the depth-age relationship with further absolute time horizons, we inspected the sulphate profile to identify volcanic horizons such as found in other northern hemisphere ice cores between 1912 AD (Katmai) and 1783 AD (Laki) in Greenland (Legrand et al., 1997; Clausen et al., 1997) and at Colle Gnifetti (Bohleber 2008). However, since Elbrus is a volcanic crater, it is sometimes difficult to attribute a peak either to a well-known global eruption or to a local event. Furthermore, numerous sulphate peaks in the Elbrus ice core originate from terrestrial input as suggested by the presence of concomitant calcium peaks. The Katmai eruption in 1912 AD could be clearly identified at 87.7 m w.e. (dated at 1911 AD

653 using the ammonium stratigraphy) with several neighbouring samples showing relatively high
654 sulphate levels (up to 1200 ppb, i.e. 25 μEq L^{-1}) compared to sulphate peaks generally present
655 in summer layers in the early 20th century. Furthermore, in contrast to neighbouring summer
656 sulphate peaks located at 87.2, 87.4, 88.0, and 89.3 m w.e., that are alkaline (see Fig. 10b), the
657 acidity of samples of the 87.7 m w.e. sulphate peak reaches 8 μEq L^{-1}. Furthermore, samples
658 located of the top part of the 87.7 m w.e. sulphate peak remain neutral in spite of a large
659 presence of calcium. Figure 11 demonstrates that the one year uncertainty in dating this
660 horizon is in excellent agreement with our annual counting.

661 We were still able to easily examine annual counting down to 113 m w.e. resulting in a
662 date of 1860 AD, but below this depth the dating becomes more uncertain (see the green line
663 in Fig. 9). Below 88 m w.e., 7 significant potential volcano horizons are suspected based on
664 their ionic balance and sulphate levels (not shown), from which at least one horizon is of local
665 origin as suggested by small stones up to 1–2 mm in the corresponding ice layer.
666 Nevertheless, a series of three narrow ionic spikes occur at 118–120 m w.e. (dated at ~1840–
667 1833 AD) where two of the spikes are characterized by an increase of sulphate and acidity (up
668 to 7.8 μEq L^{-1}, not shown) that may be related to the well-known eruptions observed in
669 Greenland that are dated to 1840 AD ± 2 years. One of these eruptions may possibly be due to
670 the Coseguina eruption in 1835 AD (Legrand et al., 1997).

671 We calculated the depth-age relationship from the depths and thicknesses of the counted
672 annual layers (Fig. 9). Despite high variability in the annual layers' thickness, the data
673 demonstrate layer thinning with depth related to the ice flow. Applying the thickness-age
674 relationship developed by Nye (Dansgaard & Johnsen, 1969) to the actual annual layer data
675 (Fig. 9) provides the mean accumulation over the whole studied time period in the ice core
676 resulting in 1.583 m of ice equivalent per year. The "Nye" curve corresponds to the depth-age
677 relationship from the Nye model with such "best fit" (constant over time) accumulation rate
678 and the glacier thickness at the drilling site (Fig. 9). The green line is the depth-age
679 relationship as suggested by Salamatin's model (Salamatin et al., 2000) with the same "best
680 fit" accumulation rate and drill site basal and surface descriptions as assumed when applying
681 Nye's model.

682 Dating based on annual layer counting of the chemical stratigraphy agrees well the 1963
683 AD time horizon that is located at the core depth of 50.7 m w.e. (dated at 1965 using the
684 ammonium stratigraphy, Fig. 10a). In addition it fits very well with the dating achieved so far
685 (i.e. core down to 106.7 m) on the base of the seasonal stratigraphy of the stable isotope

686 profile. Whereas stable isotopes predict the year 1924 at a core depth of 106.7 m, the chemical
687 stratigraphy leads to estimate the year 1926 in this depth.

688 To anchor the depth age relation with further absolute time horizons, a first inspection
689 of the sulphate profile was made in view to identify volcanic horizons as found in other
690 northern hemisphere ice cores between 1912 (Katmai) and 1783 (Laki eruption) in Greenland
691 (Legrand et al., 1997; Clausen et al., 1997) and at Colle Gnifetti (Bohleber 2008). However
692 since the Elbrus is an in active volcanic crater, it is sometimes difficult to attribute a peak
693 either to a well-known global eruption or to a local event. Furthermore, numerous sulphate
694 peaks in the Elbrus ice core originate from terrestrial inputs as suggested by the presence of
695 concomitant calcium peaks. So far, the Katmai eruption in 1912 could be clearly identified at
696 87.7 m w.e. (dated at 1911 using the ammonium stratigraphy) with several neighboured
697 samples showing relatively high sulphate levels (up to 1200 ppb, i.e. 25 μEq L^{-1}) compared to
698 those seen in sulphate peaks generally present in summer layers of the early 20th century.
699 Furthermore, as seen in Fig. 10b, in contrast to neighboured summer sulphate peaks located at
700 87.2, 87.4, 88.0, and 89.3 m w.e., that are alkaline (see Fig. 10b), the acidity of samples of the
701 87.7 m w.e. sulphate peak reaches 8 μEq L^{-1} at the bottom part of the sulphate peak.
702 Furthermore, samples located of the top part of the 87.7 m w.e. sulphate peak remains neutral
703 in spite of a large presence of calcium (similar to those seen in neighboured summer sulphate
704 peaks). As seen in Figure 9 it appears that within one-year uncertainty this horizon is in
705 excellent agreement with our annual counting.

706

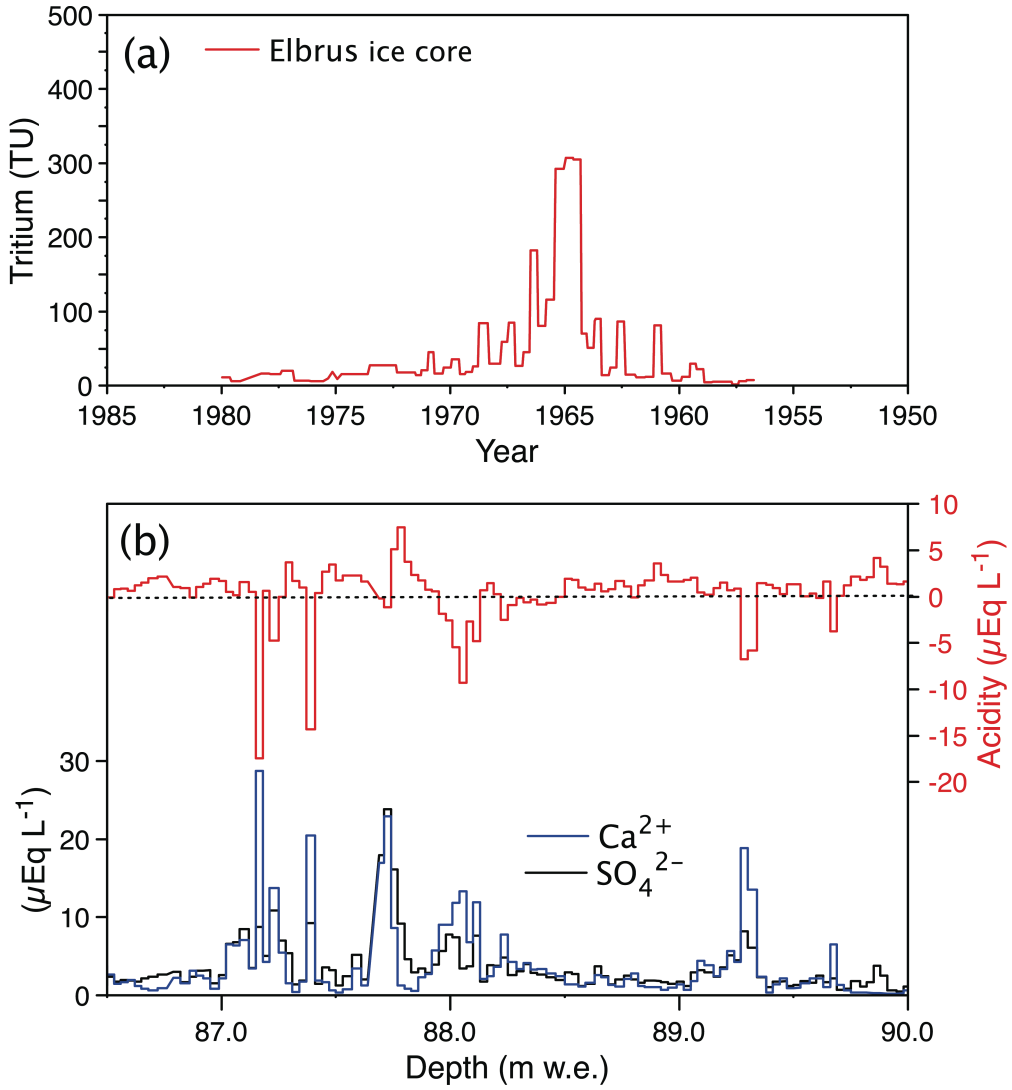

Figure 10. Absolute time horizons: (a) Tritium measurements made on Elbrus ice core samples (data were converted to 2009 with regard to the half-life time of tritium, $T_{1/2}$ = 12.32 year). The dates reported in the tritium curve are derived from the ammonium stratigraphy. (b) Calculated acidity (top, see Sect. 3.3.1), calcium and sulfate (bottom) in ice layers located between 86.5 and 90 m w.e.

Below 88 m w.e., we were still able to easily proceed annual counting down to 113 (1860), whereas further down the dating become more uncertain (see the green line in Fig. 9). Below 88 m w.e., 7 significant potential volcano horizons can be suspected on the basis of the ionic balance and sulphate levels (not shown), from which however at least 1 are of local origin (as suggested by small stones with size of up to 1–2 mm were found in the corresponding layer). Nevertheless, a series of 3 narrow spikes was located at 118–120 m w.e. (dated at around 1840–1833) among which two that are characterized by an increase of

sulphate and acidity (up to 7.8 µEq L^{-1}, not shown) may be related to the well-known eruptions observed in Greenland in a time distance of 2 years around 1840 (one of them being possibly due to the Coseguina eruption in 1835) (Legrand et al., 1997).

3.4 Modeled ice flow and ice core dating

Mountain glaciers in volcanic craters present have different thermodynamic properties than other mountain glaciers. The limited ice flux over the crater rims form flat glacier surfaces with low surface ice velocity. The intense volcanic heat flux may result in basal melting and the associated removal of the oldest basal layers. A simplified thermo-mechanically coupled model for simulating ice flow along a fixed flow tube and heat transfer in ice caps filling volcanic craters was developed by Salamatin et al. (2000). The model description and ice-flow and heat-transfer equations described in detail in Salamatin et al. (2000). The model takes into account surface and bedrock topography and snow-firn densification parameters (see section3.3.2), the distribution of the basal melt rate (see section 3.3.1) and normalizes the results by the present day accumulation rate. We calculated the depth-age relationship for the Western Elbrus Plateau using the recent accumulation rate of 1200 mm w.e. The ice melt rate at the glacier bedrock is negligible and comprises less than 10 mm w.e y^{-1} (see section3.3.1) in the deepest glacier sections. Figure 11shows the cross section of the Western Elbrus Plateau along a reference flow line. Predicted ice flow paths are shown by lines with arrows while isochrones are designated by numbers which specify the ice age in years.

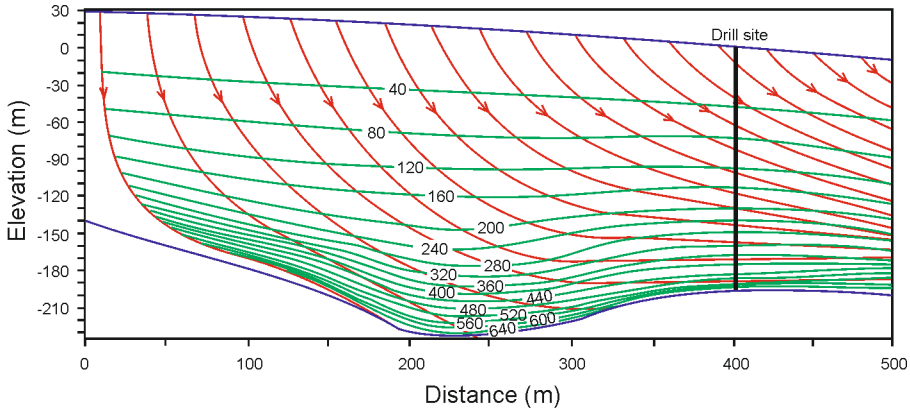

Figure 11. Vertical transect of the Western Elbrus Plateau glacier along a reference flow line. Predicted ice-particle paths (lines with arrows) and isochrones are shown.

4. Conclusions

Paleoclimatological records for southern and eastern Europe are based on geomorphological, palinological, limnological, and dendrochronological data. Ice core records have not been taken into account as a source of paleoclimate and environmental information for this area due to rapid glacier mass exchange rate and significant surface melting, often resulting in smoother isotopic and chemical profiles in glacier records. However, the deep Elbrus ice core drilled in 2009 at 5115 m a.s.l. provides new evidence for significant regional-scale multiproxy climatic implications. The negative ice temperature of the glacier at the drilling site results in an undisturbed incoming climate signal. The considerable snow accumulation rate of 1455 mm w.e. coupled with high-resolution ice core sampling allows us to separate snow seasonal climate signals from summer and winter precipitation. Annual layers were differentiated on the basis of seasonal oscillations of NH_4^+, succinic acid, and $\delta^{18}O$. Annual layer counting was confirmed by the well-known reference horizons of the 1963 AD nuclear tests and the 1912 AD Katmai volcanic eruption. Annual layer counting extends down to 85 m w.e. Ice flow models show that the basal ice age at the maximum glacier depth of 255 m is more than 600 years before present. The 2009 drilling site was situated downstream from this maximum depth location and the resulting basal ice age does not exceed 350–400 years before present. An essential difference between reported depth-age scale constructed from annual layer counting versus the age scale created from flow models requires inspecting the model algorithm and developing a reliable ice flow model.

The combination of the different glacio-chemical features of the Western Elbrus Plateau detailed in this study demonstrates that this high elevation glacier archive offers the possibility to extract atmospheric relevant information from long-term ice core records in the Caucasus. On-going research is therefore dedicated to reconstructing several key aspects of the changing atmosphere of this central European region, in particular for various aerosol components such as sulphate, ammonium, terrigenous matter, and carbonaceous compounds or fractions and species related to the nitrogen cycle.The comparison of Elbrus ice core with ice core records from Alpine glaciers (Col du Dôme and Colle Gnifetti) will allow us to estimate the tendency of climatic changes over Europe for the last few centuries, and to obtain high resolution multiproxy reconstructions of atmospheric chemistry, air temperature and precipitation oscillations, black carbon pollution, and atmospheric circulation change.

*Acknowledgments***.** The ice core recovery in 2009 was funded by the Russian Foundation for Basic Research (RFBR) Grants 07-05-00410 and 09-05-10043.V. Mikhalenko, S. Kutuzov, and I. Lavrentiev acknowledge support of the Russian Academy of Sciences (Department of Earth Sciences ONZ-12 Project) and RFBR Grant 14-05-00137. S. Sokratov acknowledges support of

the RSF (project 14-37-00038) in his contribution to the paper. The ongoing laboratory analyses at LGGE and logistics were supported by the EU FP7 IP PEGASOS (FP7-ENV- 2010/265148), the French ANR program PAPRIKA (ANR-09-CEP-005-02), the CNRS-DFG bilateral project entitled "Secondary organic aerosol production in the lower free troposphere over western Europe", and the LEFE-CHAT program ESCCARGO. Stable water isotopic analyses were supported by the RFBR Grant 14-05-31102 (A. Kozachek, A. Ekaykin, and V. Lipenkov, AARI) and IAEA Research Contracts 16184/R0 (Stable water isotopes in the cryosphere of the Northern Eurasia), and 16795 (Paleo-Climate Isotope Record from European Mt. Elbrus Ice Core). This research work was conducted in the framework of the International Associated Laboratory (LIA) "Climate and Environments from Ice Archives" 2012–2016 linking several Russian and French laboratories and institutes. Two anonymous reviewers and the editor are acknowledged for their valuable comments and suggestions to improve the manuscript. Authors thank Natalie Kehrwald for her help in tuning up the language.

References

Abich, H.: Geologische Beobachtungen auf Reisen im Kaukasus im Jahre 1873, Bulletin de la Société impériale des naturalistes de Moscou, 48(2), 278–342 + 1 Karte, 1874a.

Abich, H.: Geologische Beobachtungen auf Reisen im Kaukasus im Jahre 1873 (Fortsetzung), Bulletin de la Société impériale des naturalistes de Moscou, 48(3), 63–107, 1874b.

Abich, H.: Geologische Beobachtungen auf Reisen im Kaukasus im Jahre 1873 (Schluss), Bulletin de la Société impériale des naturalistes de Moscou, 48(4), 243–272, 1874c.

AMAP: Snow, Water, Ice and Permafrost in the Arctic (SWIPA): Climate Change and the Cryosphere, Arctic Monitoring and Assessment Programme (AMAP), Oslo, 538 pp., 2011.

Anisimov, O.A. and Zhil'tsova, E.L.: Climate change estimates for the regions of Russia in the 20th century and in the beginning of the 21st century based on the observational data, Rus. Meteorol. Hydrol., 37(6), 421–429, doi:10.3103/S1068373912060106, 2012.

Arkhipov, S.M., Mikhalenko, V.N., Thompson, L.G., Zagorodnov, V.S., Kunakhovich, M.G., Smirnov, K.E., Makarov, A.V., and Kuznetsov, M.P.: Stratigrafiya deyatel'nogo sloya lednikovogo kupola Vetrenyi na ostrove Graham Bell, Zemlya Frantsa Iosifa (Stratigraphy of the active layer of the Vetreny Ice Cap, Graham Bell Island, Franz Josef Land), Materialy glyatsiologicheskikh issledovanii (Data Glaciol. Stud.), (90), 169–186, 2001 (in Russian with English summary).

ASTER GDEM Validation Team: ASTER Global DEM Validation Summary Report, Sioux Falls, USA, 28 pp., 2009.

820 Baranov, S. and Pokrovskaya, T.: Rabota meteorologicheskoi gruppy EKNE 1935
821 (Investigations of the Meteorological team of the Elbrus Complex Scientific Expedition),
822 in: Trudy El'brusskoi ekspeditsii Akademii nauk SSSR i VIEM 1934 i 1935 gg.; Trudy
823 komissii po izucheniyu stratosfery, t. 2 (Elbrus expedition of the Academy of Sciences and
824 of the Institute of Experimental Medicine of the USSR, 1934 and 1935; Proceedings of the
825 commission of the stratosphere investigations, v. 2), resp. ed.: Vavilov, S.I., Academy of
826 Sciences Press, Moscow, Leningrad, 199–209, 1936 (in Russian with English summary).
827 Barbante, C., Schwikowski, M., Ring, T., Gäggeler, H.W., Schotterer, U., Tobler, L., Van de
828 Velde, K., Ferrari, C., Cozzi, G., Turetta, A., Rosman, K., Bolshov, M., Capodaglio, G.,
829 Cescon, P., and Bourton, C.: Historical record of European emissions of heavy metals to
830 the atmosphere since the 1650s from Alpine snow/ice cores drilled near Monte Rosa,
831 Environ. Sci. Technol., 38(15), 4085–4090, doi:10.1021/es049759r, 2004.
832 Bazhev, A.B. and Bazheva, V.Ya.: Stroenie firnovo-ledyanoy tolschi na El'bruse (Structure and
833 firn-ice layer at the south slope of Elbrus), Materialy glyatsiologicheskikh issledovanii (Data
834 Glaciol. Stud.), (10), 94–100, 1964 (in Russian with English summary).
835 Bazhev, A.B., Rototaeva, O., Heitzenberg, J., Stenberg, M., and Pinglot, J.F.: Physical and
836 chemical studies in the region of the southern slope of Mount Elbrus, Caucasus, J. Glaciol.,
837 44(147), 214–222, 1998.
838 Bender, M. Sowers, T., and Brook, E.: Gases in ice cores, P. Natl. Acad. Sci. USA, 94(16),
839 8343–8349, doi:10.1073/pnas.94.16.8343, 1997.
840 Berikashvili, V.Sh., Vasilenko, E.V., Macheret, Yu.Ya., and Sokolov, V.G.: Odnoimpulsnyi
841 radar dlya zondirovaniya lednikov s opticheskim kanalom sinkhronizatsii (Monopulse
842 radar for glacier sounding with optical channel for synchronization and digital signal
843 processing), Radiotekhnika (Radio technics), (9), 52–57, 2006 (in Russian with English
844 summary).
845 Bohleber, P.: Age distribution and $\delta^{18}O$ variability in a low accumulation Alpine ice core:
846 Perspective for paleoclimate studies, Diploma thesis, Fakultät für Physik und Astronomie,
847 Ruprecht-Karls-Universität, Heidelberg, 147 pp., 2008.
848 Clausen, H.B., Hammer, C.U., Hvidberg C.D., Dahl-Jensen, D., Kipfstuhl, J., and Legrand, M.:
849 A comparison of the volcanic records over the past 4000 years from the Greenland Ice Core
850 Project and Dye 3 Greenland ice cores, J. Geophys. Res., 102(C12), 26707–26723,
851 doi:10.1029/97JC00587, 1997.
852 Dansgaard, W., Johnsen, S.J. A flow model and a time scale for the ice core from Camp Century,
853 Greenland, J.Glaciol., 8(53),215–223, 1969.

Dolgova E.A., Matskovskii V.V., Solomina O.N., Rototarva O.V., Nosenko G.A., and Khmelevskoi I.F.: Rekonstruktsiya balansa massy lednika Garabashi (1800–2005) po dendrokhronologicheskim dannym (Reconstructing mass balance of Grabashi Glacier (1800–2005) using dendrochronological data), Led i Sneg (Ice and Snow), 53(1), 34–42, doi:10.15356/2076-6734-2013-1-34-42, 2013 (in Russian with English summary).

Dyurgerov, M.B. and Popovnin, V.V.: Rekonstruktsiya balansa massy, prostranstvennogo polozheniya i zhidkogo stoka lednika Dhzankuat so vtoroi poloviny 19 veka (Reconstruction of mass balance, spatial position, and liquid discharge of Dzhankuat Glacier since the second half of the 19th century), Materialy glyatsiologicheskikh issledovanii (Data Glaciol. Stud.), (40), 111–126, 1988 (in Russian with English summary).

Eichler, A., Tinner, W., Brusch, S., Olivier, S., Papina, T., and Schwikowski, M.: An ice-core based history of Siberian forest fires since AD 1250, Quaternary Sci. Rev., 30(9–10), 1027–1034, doi:10.1016/j.quascirev.2011.02.007, 2011.

Fagerli H., Legrand, M., Preunkert, S., Vestreng, V., Simpson, D., and Cerquera, M.: Modeling historical long-term trends of sulfate, ammonium, and elemental carbon over Europe: A comparison with ice core records in the Alps. J. Geophys. Res., 112(D23), D23S13: 1–16, doi:10.1029/2006JD008044, 2007.

Ginot, P., Schotterer, U., Stichler, W., Godoi, M. A., Francou, B., and Schwikowski, M.: Influence of the Tungurahua eruption on the ice core records of Chimborazo, Ecuador, The Cryosphere, 4(4), 561–568, doi:10.5194/tc-4-561-2010, 2010.

Golubev, G.N., Dyurgerov, M.B., Markin, V.A., Berry, B.L., Sukhanov, L.A., Zolotarev, E.A., Danilina, A.V., and Arutyunov, Yu.G.: Lednik Dzhankuat (Tsentral'nyi Kavkaz) (Water-ice and heat balances of Dzankuat Glacier (Central Caucasus)), edited by: Byarski, I,Ya., Hydrometeoizdat Press, Leningrad, 184 pp., 1978 (in Russian with English summary).

Golubev, V.N., Mikhalenko, V.N., Serebrennikov, A.V., and Gvozdik, O.A.: Strukturnye issledovaniya ledyanogo kerna Dzhantuganskogo firnovogo plato na Tsentral'nom Kavkaze (Structural studies of the ice core obtained from the Djantugan Firn Plateau in the Central Caucasus), Materialy glyatsiologicheskikh issledovanii (Data Glaciol. Stud.), (64), 25–33, 1988 (in Russian with English summary).

Hörhold, M.W., Kipfstuhl, S., Wilhelms, F., Freitag, J., and Frenzel, A.: The densification of layered polar firn, J. Geophys. Res., 116(F1), F01001: 1–15, doi:10.1029/2009JF001630, 2011.

887 Hou, S., Chappellaz, J., Raynaud, D., Masson-Delmotte, V., Jouzel, J., Bousquet P., and
888 Hauglustaine D.: A new Himalayan ice core CH_4 record: possible hints at the preindustrial
889 latitudinal gradient, Clim. Past, 9(6), 2549–2554, doi:10.5194/cp-9-2549-2013, 2013.
890 Johnsen, S., Clausen, H.B., Cuffey, K.M., Hoffmann, G., Schwander, J., and Creyts, T.:
891 Diffusion of stable isotopes in polar firn and ice: the isotope effect in firn diffusion, in:
892 Physics of Ice Core Records, edited by Hondoh, T., Hokkaido University Press, Sapporo,
893 121–140, doi:10.7916/D8KW5D4X, 2000.
894 Kawamura, K., Izawa, Y., Mochida, M., and Shiraiwa, T.: Ice core records of biomass
895 burning tracers (levoglucosan and de-hydroabietic, vanillic and p-hydroxybenzoic acids)
896 and total organic carbon for past 300 years in the Kamchatka Peninsula, Northeast Asia,
897 Geochim. Cosmochim. Ac., 99, 317–329, doi:10.1016/j.gca.2012.08.006, 2012.
898 Kerimov, A.M., Rototaeva, O.V., and Khmelevskoi, I.F.: Raspredelenie tyazhelykh metallov
899 v poverkhnostnykh sloyakh snezhno-firnovoi tolshchi na yuzhnom sklone El'brusa
900 (Distribution of heavy metals in the surface layers of snow-firn mass on the southern slope
901 of Mount Elbrus), Led i Sneg (Ice and Snow), 51(2), 24–34, doi:10.15356/2076-6734-
902 2011-2-24-34, 2011 (in Russian with English summary).
903 Kotlyakov, V.M., Arkhipov, S.M., Henderson, K.A., and Nagornov, O.V.: Deep drilling of
904 glaciers in Eurasian Arctic as a source of paleoclimatic records, Quaternary Sci. Rev.,
905 23(11–13), 1371–1390, doi:10.1016/j.quascirev.2003.12.013, 2004.
906 Kovalev P.V.: Sovremennoe oledenenie basseina reki Baksan (Recent glaciation of the
907 Baksan River basin), in: Materialy Kavkazskoi ekspeditsii (po programme
908 Mezhdunarodnogo geofizicheskogo goda) (Proc. of the Caucasus expedition (by the
909 programme of the International Geophysical Year)), v. 2, edited by: Dubinskii G.P.,
910 Khar'kov University, Khar'kov, 3–106, 1961 (in Russian).
911 Krenke, A.N., Menshutin, V.V., Voloshina, A.P., Panov, V.D., Bazhev, A.B., Bazheva, V.Ja.,
912 Balaeva, V.A., Vinogradov, O.N., Voronina, L.S., Garelik. I.S., Davidovich, N.V.,
913 Dubinskaya, N.M., Macheret, Yu.Ya., Moiseeva, G.P., Psareva, T.V., Tyulina, T.Yu.,
914 Freidlin, V.S., Khmelevskoy, I.F., Chernova, L.P., and Shadrina, O.V.: Lednik Marukh
915 (Zapadnyi Kavkaz) (Marukh Glacier (Western Caucasus)), edited by: Kotlyakov, V.M.,
916 Hydrometeoizdat Press, Leningrad, 254, 1988 (in Russian with English summary).
917 Kutuzov S., Lavrentiev, I. I., Macheret, Yu, Ya., and Petrakov, D. A.: Izmenenie lednika
918 Marukh s 1945 po 2011 (Changes of Marukh Glacier from 1945 to 2011), Led i Sneg (Ice
919 and Snow), 52(1), 123–127, doi:10.15356/2076-6734-2012-1-123-127, 2012 (in Russian
920 with English summary)

921 Kutuzov S.S., Lavrentiev I.I., Vasilenko E.V., Macheret Y.Y., Petrakov D.A., and Popov
922 G.V.: Otsenka ob'yema lednikov Bolshogo Kavkaza po dannym radiozondirovaniya i
923 modelirovaniya (Estimation of the Greater Caucasus glaciers volume, using radio-echo
924 sounding data and modelling), Kriosfera Zemli (Earth's Cryosphere), 19(1), 78–88, 2015
925 (in Russian with English summary)
926 Kutuzov, S., Shahgedanova, M., Mikhalenko, V., Lavrentiev, I, and Kemp, S.: Desert dust
927 deposition on Mt. Elbrus, Caucasus Mountains, Russia in 2009–2012 as recorded in snow
928 and shallow ice core: high-resolution "provenancing", transport patterns, physical
929 properties and soluble ionic composition, The Cryosphere, 7(5), 1481–1498,
930 doi:10.5194/tc-7-1481-2013, 2013.
931 Laverov, N.P., Dobretsov, N.L., Bogatikov, O.A., Bondur, V.G., Gurbanov, A.G.,
932 Karamurzov, B.S., Kovalenko, V.I., Melekestsev, I,V., Nechaev, Yu.V., Ponomareva,
933 V.V., Rogozhin, E.A., Sobisevich, A.L., Sobisevich, L.E., Fodotov, S.A., Khrenov, A.P.,
934 and Yarmolyuk, V.V.: Noveishii i sovremennyi vulkanizm na territorii Rossii (Modern and
935 Holocene volcanism in Russia), Nauka, Moscow, 604 pp., 2005 (in Russian with English
936 summary).
937 Lavrentiev, I.I., Mikhalenko, V.N., and Kutuzov, S.S.: Tolshchina l'da i podlednyi rel'ef
938 Zapadnogo lednikovogo plato El'brusa (Ice thickness and subglacial relief of the Western
939 Ice Plateau of Elbrus), Led i Sneg (Ice and Snow), 50(2), 12–18, doi:10.15356/2076-6734-
940 2010-2-12-18, 2010 (in Russian with English summary).
941 Legrand M., C. Hammer, M. De Angelis, J. Savarino, R. Delmas, H. Clausen, and S.J. Johnson,
942 Sulphur containing species (MSA and SO_4) over the last climatic cycle in the GRIP (central
943 Greenland) ice core, J. Geophys. Res., 102(C12), 26663–26679, doi:10.1029/97JC01436,
944 1997.
945 Legrand, M. and Mayewski, P.: Glaciochemistry of polar ice cores: A review, Rev. Geophys.,
946 35(3), 219–243, doi:10.1029/96RG03527, 1997.
947 Legrand, M., Preunkert, S., Schock, M., Cerqueira, M., Kasper-Giebl, A., Afonso, J., Pio, C.,
948 Gelencsér, A. and Dombrowski-Etchevers, I.: Major 20th century changes of carbonaceous
949 aerosol components (EC, WinOC, DOC, HULIS, carboxylic acids, and cellulose) derived
950 from Alpine ice cores, J. Geophys. Res., 112(D23), D23S11, doi:10.1029/2006JD008080,
951 2007a.
952 Legrand, M., S. Preunkert, Oliveira, T., Pio, C.A., Hammer, S., Gelencsér, A., Kasper-Giebl, A.,
953 and Laj, P.: Origin of C_2–C_5 dicarboxylic acids in the European atmosphere inferred from
954 year-round aerosol study conducted at a west-east transect, J. Geophys. Res.,112(D23),
955 D23S07, doi:10.1029/2006JD008019, 2007b.

956 Ligtenberg, S.R.M., Helsen, M.M., and van den Broeke, M.R.: An improved semi-empirical
957 model for the densification of Antarctic firn, The Cryosphere, 5(4), 809–819,
958 doi:10.5194/tc-5-809-2011, 2011.
959 Looyenga, M.: Dielectric constant of heterogeneous mixtures, Physica, 31(3), 401–406,
960 doi:10.1016/0031-8914(65)90045-5, 1965.
961 Macheret, Yu.Ya.: Radiozondirovanie lednikov (Radio-echo sounding of glaciers), Scientific
962 World Publishers, Moscow, 392 pp., 2006 (in Russian with English summary).
963 Maeno, N. and Ebinuma, T.: Pressure sintering of ice and its implication to the densification
964 of snow at polar glaciers and ice sheets, J. Phys. Chem., 87(21), 4103–4110,
965 doi:10.1021/j100244a023, 1983.
966 Matyukhin, G.D.: Klimaticheskie dannye po vysotnym poyasam yuzhnogo sklona El'brusa
967 (Climatic data for the southern slope of Elbrus), in: Informatsionnyi sbornik o rabotakh po
968 Mezhdunarodnomu geofizicheskomu godu (Information collection on the investigations in
969 International Geophysical Year), 5, Faculty of Geography, Moscow State University,
970 Moscow, 130–194, 1960 (in Russian).
971 Mätzler, C. and Wegmüller, U.: Dielectric properties of fresh-water ice at microwave
972 frequencies, J. Phys. D Appl. Phys., 20(12), 1623–1630, doi:10.1088/0022-
973 3727/20/12/013, 1987.
974 Mikhalenko, V.N., Kuruzov, S.S., Lavrentiev, I.I., Kunakhovich, M.G., and Thompson, L.G.:
975 Issledovanie zapadnogo lednikovogo plato El'brusa: rezul'taty i perspektivy (Western
976 Elbrus Plateau studies: results and perspectives), Materialy glyatsiologicheskikh issledovanii
977 (Data Glaciol. Stud.), (99), 185–190, 2005 (in Russian with English summary)
978 Mikhalenko, V.N.: Glubinnoe stroenie lednikov tropicheskikh i umerennykh shirot (Inner
979 structure of glaciers in non-polar regions), LKI Publishers, Moscow, 320 pp., 2008 (in
980 Russian with English summary).
981 Mikhalenko, V.N.: Glubokoe burenie l'la bliz vershiny El'brusa (Deep ice core drilling near
982 summit of Mt. Elbrus), Led i Sneg (Ice and Snow), 50(1), 123–126, doi:10.15356/2076-
983 6734-2010-1-123-126, 2010 (in Russian with English summary).
984 Mushketov, I.V.: Geologicheskaya poezdka na Kavkaz v 1881 (Geological excursion to the
985 Caucasus in 1881), Izvestiya Imperatorskogo Russkogo geograficheskogo obshchestva
986 (Proc. Rus. Geogr. Soc.), 18(2), 106–119, 1882 (in Russian).
987 Nosenko, G.A., Khromova, T.E., Rototaeva, O.V., and Shahgedanova, M.: Reaktsiya
988 lednikov Tsentral'nogo Kavkaza v 2001–2010 na izmeneniya temperatury i kolichestva
989 osadkov (Glacier reaction to temperature and precipitation change in Central Caucasus),

2001–2010, Led i Sneg (Ice and Snow), 1(121), 26–33, doi:10.15356/2076-6734-2013-1-26-33, 2013 (in Russian with English summary).

Pastukhov, A.V.: Poseshchenie El'brusa 13 iyulya 1890 (Ascending to Elbrus on 13 July, 1890), Zapiski Kavkazskogo otdela Imperatorskogo Russkogo geograficheskogo obshchestva (Mem. Cauc. branch Imperial Rus. Geogr. Soc.), 15, 22–37, 1893 (in Russian).

Podozerskii, K.I.: Ledniki Kavkazskogo khrebta (Glaciers of the Caucasus Range), Zapiski Kavkazskogo otdela Imteratorskogo Russkogo geograficheskogo obschestva (Mem. Cauc. branch Imperial Rus. Geogr. Soc.), 29(1), 200 pp., 1911 (in Russian).

Preunkert, S. and Legrand, M.: Towards a quasi-complete reconstruction of past atmospheric aerosol load and composition (organic and inorganic) over Europe since 1920 inferred from Alpine ice cores, Clim. Past, 9(4), 1403–1416, doi:10.5194/cp-9-1403-2013, 2013.

Preunkert, S., Wagenbach, D., Legrand, M., and Vincent, C.: Col du Dôme (Mt Blanc Massif, French Alps) suitability for ice-core studies in relation with past atmospheric chemistry over Europe, Tellus, 52B(3), 993–1012, doi:10.1034/j.1600-0889.2000.d01-8.x, 2000.

Psareva, T.V.: Preobrazovanie snezhno-firnovoi tolshchi i tipy l'doobrazovaniya na El'bruse (Transformation of snow-firn thickness and types of ice formation on Elbrus), Materialy glyatsiologicheskikh issledovanii (Data Glaciol. Stud.), (10), 79–86, 1964 (in Russian with English summary).

Rototaeva, O.V. and Tarasova, L.N.: Rekonstruktsiya balansa massy lednika Garabashi za poslednee stoletie (Reconstruction of the Garabashi Glacier mass balance in the last century), Materialy glyatsiologicheskikh issledovanii (Data Glaciol. Stud.), (88), 16–26, 2000 (in Russian with English summary).

Rototaeva, O.V., Nosenko, G.A., Tarasova, L.N., and Khmelevskoy, I.F.: Obschaya kharakteristika oledeneniya severnogo sklona Bol'shogo Kavkaza (General characteristics of glaciation of the north slope of the Greater Caucasus), in: Sovremennoe oledenenie Severnoi i Tsentral'noi Evrazii (Glaciation in North and Central Eurasia at present time), edited by: Kotlakov, V.M., Nauka Press, Moscow, 141–144, 2006 (in Russian).

Salamatin, A.N., Lipenkov, V.Ya., Barnola, J.-M., Hori, A., Duval, P., and Hondoh T.: Snow/firn densification in polar ice sheets, in: Physics of Ice Core Records II: Papers collected after the 2nd International Workshop on Physics of Ice Core Records, held in Sapporo, Japan, 2–6 February 2007 (Low Temperature Science; 68(Suppl.)), edited by: Hondoh, T., Sapporo, Institute of Low Temperature Science, Hokkaido University, 195–222, 2009.

Salamatin, A.N., Murav'yev, Y.D., Shiraiwa, T., and Matsuoka, K.: Modelling dynamics of glaciers in volcanic cratrs, J. Glaciol., 46(153), 177–187, doi:10.3189/172756500781832990,

2000.
Salamatin, A.N., Shiraiwa, T., Muravyev, Y.D., Kameda, T., Silantiyeva, E., and Ziganshin, M.: Dynamics and borehole temperature memory of Gorshkov Ice Cap on the summit of Ushkovsky Volcano, Kamchatka Peninsula, Proceedings of the International Symposium on the Atmosphere-Ocean-Cryosphere Interaction in the Sea of Okhotsk and the Surrounding Environments held at Institute of Low Temperature Science, Hokkaido University, Sapporo, Japan, December 12–15, 2000, 120–121, 2001.
Sato, T., Shiraiwa, T., Greve, R., Seddik, H., Edelmann, E., and Zwinger, T.: Accumulation reconstruction and water isotope analyses for 1736–1997 of an ice core from the Ushkovsky volcano, Kamchatka, and their relationships to North Pacific climate records, Clim. Past, 10(1), 393–404, doi:10.5194/cp-10-393-2014, 2014.
Schwikowski, M.: Reconstruction of European air pollution from Alpine ice cores, in: Earth Paleoenvironments: Records Preserved in Mid- and Low-Latitude Glaciers, edited by: DeWayne Cecil, L., Green, J.R., Thompson, L.G., Developments in Paleoenvironmental Research, 9, Kluwer Academic Publishers, 95–119, doi:10.1007/1-4020-2146-1_6, 2004.
Serebryannyi, L.R., Golodkovskaya, N.A., Orlov, A.V., Malyasova, E.S., and Il'ves, E.O.: Kolebaniya lednikov i protsessy morenonakopleniya na Tsentral'nom Kavkaze (Glacier variations and moraine accumulation: processes in Central Caucasus), Nauka, Moscow, 216 pp., 1984 (in Russian with English summary).
Shahgedanova M., Nosenko G., Kutuzov S., Rototaeva O., and Khromova T.: Deglaciation of the Caucasus Mountains, Russia/Georgia, in the 21st century observed with ASTER satellite imagery and aerial photography, The Cryosphere, 8(6), 2367–2379, doi:10.5194/tc-8-2367-2014, 2014.
Shahgedanova, M., Kutuzov, S., White, K., and Nosenko, G.: Using the significant dust deposition event on the glaciers of Mt. Elbrus, Caucasus Mountains, Russia on 5 May 2009 to develop a method for dating and provenancing of desert dust events recorded in snow pack, Atmos. Chem. Phys., 13(4), 1797–1808, doi:10.5194/acp-13-1797-2013, 2013.
Solomina O.N., Kalugin, I.A., Aleksandrin, M.Yu., Bushueva, I.S., Darin, A.V., Dolgova, E.A., Jomelli, V., Ivanov, M.N., Matskovsky, V.V., Ovchinnikov, D.V., Pavlova, I.O., Razumovsky, L.V., and Chepurnaya, A.A.: Burenie osadkov ozera Kara-Kel' (dolina reki Teberdy) i perspektivy rekonstruktsii istorii oledeneniya i klimata golotsena na Kavkaze (Coring of Karakel' Lake sediments (Teberda River valley) and prospects for reconstruction of glaciation and Holocene climate history in the Caucasus), Led i Sneg (Ice and Snow), 53(2), 102–111, doi:10.15356/2076-6734-2013-2-102-111, 2013 (in Russian with English summary).

Solomina, O.N., Dolgova, E.A., and Maximova, O.E.: Rekonstruktsiya gidrometeorologicheskikh uslovii poslednikh stoletii na severnom Kavkaze, v Krymu i na Tyan' Shane po dendrokhronologicheskim dannym (Tree-ring based hydrometeorological reconstructions in the Crimea, the Caucasus and Tien-Shan), Nestor History Press, Moscow, St. Petersburg, 232 pp., 2012 (in Russian with English summary).

Stokes, C.R., Gurney, S.D., Shahgedanova, M, and Popovnin, V.: Late-20th-century changes in glacier extent in the Caucasus Mountains, Russia/Georgia, J. Glaciol., 52(176), 99–109, doi:10.3189/172756506781828827, 2006.

Takeuchi, N., Takahashi, A., Uetake, J., Yamazaki, T., Aizen, V. B., Joswiak, D., Surazakov, A. and Nikitin, S.: A report on ice core drilling on the western plateau of Mt. Belukha in the Russian Altai Mountains in 2003, Polar Meteorol. Glaciol., 18, 121–133, 2004.

Thompson, L.G.: Understanding Global Climate Change: Paleoclimate Perspective from the World's Highest Mountains, Proc. Amer. Phil. Soc., 154(2), 133–157, 2010.

Troshkina, E.S.: Stratigrafiya snazhno-firnovogo pokrova v oblasti pitaniya (Snow and firn stratigraphy in the accumulation zone of the Mt. Elbrus), in: Oledenenie El'brusa (Elbrus Glaciation), edited by Tushinskii, G.K., Moscow University Press, Moscow, 213–222, 1968 (in Russian).

Tushinskii, G.K. (ed.): Oledenenie El'brusa (Glaciation of the Elbrus Mountain), Moscow University Press, Moscow, 346 pp., 1968 (in Russian)

Vasilenko, E.V., Glazovsky, A.F., Macheret, Yu.Ya., Navarro, F., Sokolov, V.G., and Shiraiwa, T.: Georadar VIRL dlya zondirovaniya lednikov (Georadar VIRL for glacier sounding), Materialy glyatsiologicheskikh issledovanii (Data Glaciol. Stud.), (94), 225–234, 2003 (in Russian with English summary).

Vasilenko, E.V., Sokolov, V.A., Macheret, Y., Glazovsky, A.F., Cuadrado, M.L., and Navarro, F.J.: A digital recording system for radioglaciological studies, Bull. R. Soc. N. Z.,35, 611–617, 2002.

Vaughan, D.G., Comiso, J.C., Allison, I., Carrasco, J., Kaser, G., Kwok, R., Mote, P., Murray, T., Paul, F., Ren, J., Rignot, E., Solomina, O., Steffen, K., and Zhang, T.: Observations: Cryosphere, in: Climate Change 2013: The Physical Science Basis. Contribution of Working Group I to the Fifth Assessment Report of the Intergovernmental Panel on Climate Change, edited by: Stocker, T.F., Qin, D., Plattner, G.-K., Tignor, M., Allen, S.K., Boschung, J., Nauels, A., Xia, Y., Bex, V., and Midgley, P.M., Cambridge University Press, Cambridge, United Kingdom and New York, NY, USA, 317–382, 2013.

Vimeux, F., Ginot, P., Schwikowski, M., Vuille, M., Hoffmann, G., Thompson, L. G., and Schotterer, U.: Climate variability during the last 1000 years inferred from Andean ice

cores: A review of methodology and recent results, Palaeogeogr., Palaeoclimatol., Palaeoecol., 281(3–4), 229–241, doi:10.1016/j.palaeo.2008.03.054, 2009.

Volodicheva, N.: The Caucasus, in: The Physical geography of Northern Eurasia, edited by: Shahgedanova, M., Oxford University Press, Oxford, 350–376, 2002.

Werner, M., Mikolajewicz, U., Heimann, M., and Hoffmann, G.: Borehole versus isotope temperatures on Greenland: Seasonality does matter, Geophys. Res. Lett., 27(5), 723–726, doi:10.1029/1999GL006075, 2000.

Zagorodnov, V.S., Arkhipov, S.M., Bazhev, A.B., Vostokova, T.A., Korolev, P.A., Rototaeva, O.V., Sinkevich, S.A., and Khmelevskoy, I.F.: Stroenie, sostav i gidrotermicheskii rezhim lednika Garabashi na El'bruse (Structure, state and hydrothermal regime of the Garabashi Glacier, the Elbrus area), Materialy glyatsiologicheskikh issledovanii (Data Glaciol. Stud.), (73), 109–117, 1992 (in Russian with English summary).

Zagorodnov, V.S., Nagornov, O.V., and Thompson, L.G.: 2006. Influence of air temperature on a glacier's active-layer temperature. Ann. Glaciol., 43, 285–287, doi:10.3189/172756406781812203, 2006.

Zolotarev, E.A.: Evolutsiya oledeneniya El'brusa: katrografo-aerokosmicheskie tekhnologii glyatsiologicheskogo monitoringa (Evolution of Elbrus glaciers: Cartographic-aerospace technologies of glacier monitoring), Nauchnyi Mir, Moscow, 238 pp., 2009 (in Russian).

Zolotarev, E.A. and Khar'kovets, E.G.: Oledenenie El'brusa v kontse XX veka: tsifrovaya ortofotokarta El'brusa na 1997 (Glaciation of Elbrus at the end of XX century (digital orthophotomap of Elbrus for 1997)), Materialy glyatsiologicheskikh issledovanii (Data Glaciol. Stud.), (89), 175–191, 2000 (in Russian with English summary).

Zolotarev, E.A. and Khar'kovets, E.G.: Evolutsiya oledeneniya El'brusa posle malogo lednikovogo perioda (Development of glaciers of Mount Elbrus after the Little Ice Age), Led i Sneg (Ice and Snow), 52(2), 15–22, doi:10.15356/2076-6734-2012-2-15-22, 2012 (in Russian with English summary).